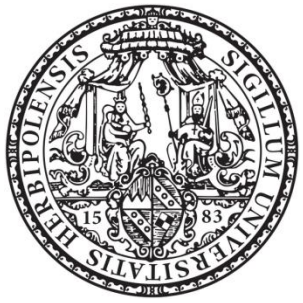

Julius-Maximilian's University of Wuerzburg
Faculty of Computer Science
Institute of Robotics and Telematics

Design of radiation tests for Photonic Mixer Device (PMD) based Imaging Sensor

Master thesis in the subject
Space Science and Technology

Presented by
Vishnu anand Muruganandan

Julius-Maximilian's University of Wuerzburg
Informatics VII
Institute of Robotics and Telematics

Design of radiation test for Photonic Mixer Device (PMD) based Imaging Sensor

Master thesis in the subject
Space Science and Technology

Presented by
Vishnu anand Muruganandan

Completed at
University of Wuerzburg
Institute of Robotics and Telematics

Guided by
Prof. Dr. rer. nat Klaus Schilling
Prof. Dr. Andreas Nuechter

Supervised by
MSc. Karthik Ravandoor
MSc. Julian Scharnagl

Acknowledgment

It's always fascinating whenever I look at the night sky that was the point I became curious about the infinite space. I'm happy to share the information in this document with everyone. My thoughts are full of radiation for past seven months. The ideas and the structured work presented in this document are not possible without my supervisors, who have always motivated me to expand the territory. I thank my supervisors Mr. Karthik Ravandoor and Mr. Julian Scharnagl for guiding throughout the process.

I like to thank Prof. Klaus Schilling for giving me an opportunity to work in a real time project and for always guiding me to bring out the best. I also like to thank Prof. Dr. Andreas Nuechter for accepting to be the guide. My special thanks to Mr. Stephan Busch who directed me towards radiation testing for space components in Team Design Project. I will be always respectful to all my faculties of Space Master Program and University of Wuerzburg, which have been wonderful experience forever. All my friends have been a great support throughout this Master's program; I dedicate this work to them.

At last my parents without them this moment is not possible. They always given me the freedom to choose the way and they gave everything to go along with my dreams.

Declaration

I hereby declare that this submission is my own work and that, to the best of my knowledge and belief, it contains no material previously published or written by another person nor material which to a substantial extent has been accepted for the award of any other degree or diploma of the university or other institute of higher learning, except where due acknowledgement has been made in the text.

Wuerzburg, the 25th, August 2014

_____

(Vishnu Anand Muruganandan)

Abstract

There are numerous charged particles (protons, electrons) revolving around the earth at magnetosphere. Highly charged particles are emitted during solar storms and eruptions. At the poles, heavy ions from Galactic Cosmic Rays (GCR) are dominant during solar minimum cycle. The satellites around the earth are always vulnerable to these charged particles. It causes various radiation effects in the satellite components. The energy, flux and fluent of these charged particles varies based on the altitude and inclination of the orbit. It also depends on solar cycle (solar minimum and maximum) of the year.

Based on the technology and design, the component can be hardened to overcome the radiation effects. The PMD (Photonic Mixer Device) 3D image sensor is planned to use for rendezvous and docking (RVD) maneuvers, to obtain the distance information of the object. But the PMD sensor is a commercial component, which is not designed and fabricated for space application. The aim of this thesis is to evaluate the survivability of the PMD image sensor for orbital operations. Using SPENVIS (Space Environment Information System) software, radiation sources and their effects in target orbit is estimated. Also from the information of previous space missions, total dose exposed on the object in orbit is predicted.

The Total Ionizing Dose (TID) testing is planned at irradiation facility. The total dose for exposure, dose rate, and number of samples required and the radiation testing procedure is planned. To measure the quality of sensor during the irradiation, the test case is designed. The test case lists the parameters (performance of the pixel and sensor) which have to be monitored during the testing. The methodologies for measuring those parameters are described. The component is qualified if the parameters don't exceed the maximum value during the irradiation and annealing. The future tasks for the implementation of radiation testing are discussed.

Table of Contents

List of Tables

List of Figures

1. Introduction

The radiation in space is generated by charged particles from various sources. The charged particles are produced by various sources from both within and beyond our solar system. The satellites in orbit are always exposed to radiation from various sources. The flux, fluence, and energy of the particle varies according to the altitude and inclination of the orbit above earth atmosphere. The radiation effects from these particles not only cause degradation but can also cause failure of electronics and electrical system of satellite. It can be overcome either by using radiation hardened devices or qualifying commercial devices by radiation ground testing. The radiation hardened devices are reliable for space application. The problem is hardened devices are expensive, less available and fabricated using non state of art technologies.

The COTS (Commercially of the shelf) components are affordable and accessible by private space organizations. But the COTS components are not designed for space application. It is vulnerable to radiation effects. The Photonic Mixer Device (PMD) is a 3D image sensor, it's a commercial device and it's not hardened for space application. It is planned to be used in the satellite operations. To qualify this component, first the exposure of radiation at orbit is estimated by SPENVIS (Space Environment Information System) software. Then the commercial component is qualified by radiation ground testing to determine if the component will survive in the radiation environment of the target orbit. The charged particles exposed to the target orbit, duration of the mission, design and manufacturing technology of the component are considered while implementing the radiation testing in the lab. Based on the results of radiation testing, it's analyzed if the component will survive in the particular orbit of interest.

1.1 Thesis definition

The primary idea of the thesis is to test the radiation tolerance (ground testing) of the PMD PhotonICs 19k-S3 image sensor (3D chip). The image sensor is based on the CMOS technology. This 3D image sensor is evaluated for future orbital operation, which might be similar to DEOS (Deutsche Orbital Servicing Mission). DEOS is a typical on-orbit servicing mission. Hence the DEOS orbital configuration is assumed for the estimation of radiation exposure on the component. The configuration of the DEOS orbit are inclination = 90º, perigee = 400 km, apogee = 600 km. The following steps are taken in order to confirm the reliability of the sensor in the target orbit.

i) Theoretical study about the PMD sensor, radiation environment of the target orbit and various radiation effects.
ii) Estimation of the total dose exposed to semi-conductor in orbit using spenvis radiation model and comparing the results of spenvis with previous orbital experiences in radiation exposure.

iii) Determination of required shielding for the component in the orbit.
iv) Estimating the total dose and dose rate for the irradiation test set up
v) Designing the test case and evaluation of the component by parameters measurements.

1.2 Report outline

The structure of the report is described in following;

i) Introduction: Brief idea about the background of thesis and objectivity.
ii) Theory: Detailed description about the radiation sources, effects and PMD sensor. The information from previous space missions related to radiation exposure
iii) Spenvis radiation modal: Estimation of TID (Total Ionizing Dose) by radiation model.
iv) Design of the radiation test set up: Estimation of dose rate, test case for parameters measurement.
v) Conclusion: summary and future tasks for the implementation of radiation testing.

2. Theory

This chapter contains three sections. First the basic operating principle and the components of PMD sensor are described, which is to be tested in the radiation environment. The next section list the characteristics of various radiation sources exposed to satellites in the orbit. The following section describes different radiation effects on various components. It is important to discuss about the radiation source and effects. The type of radiation and amount of exposure varies according to the orbit and the radiation effects are based on the orbit and technology of the component. In final section, the orbital experiences regarding the radiation level (doses) exposed on satellites and previous radiation testing on image sensor is discussed.

2.1 Photonic Mixer Device (PMD) Sensor

The PMD PhotonICs 19k-S3 is a 3-d image sensor. The main objective of the thesis is to qualify this PMD sensor during radiation testing for space operation. The PMD sensor is based on Time of Flight (TOF) principle. In brief, a light is transmitted towards an object and distance to the object is calculated from the time taken to reflect back to the receiver, since the velocity of light is constant. Each pixel in the image sensor detects the brightness and depth (distance) of the image, hence it's known as smart pixel. The operation of PMD camera system is explained in following.

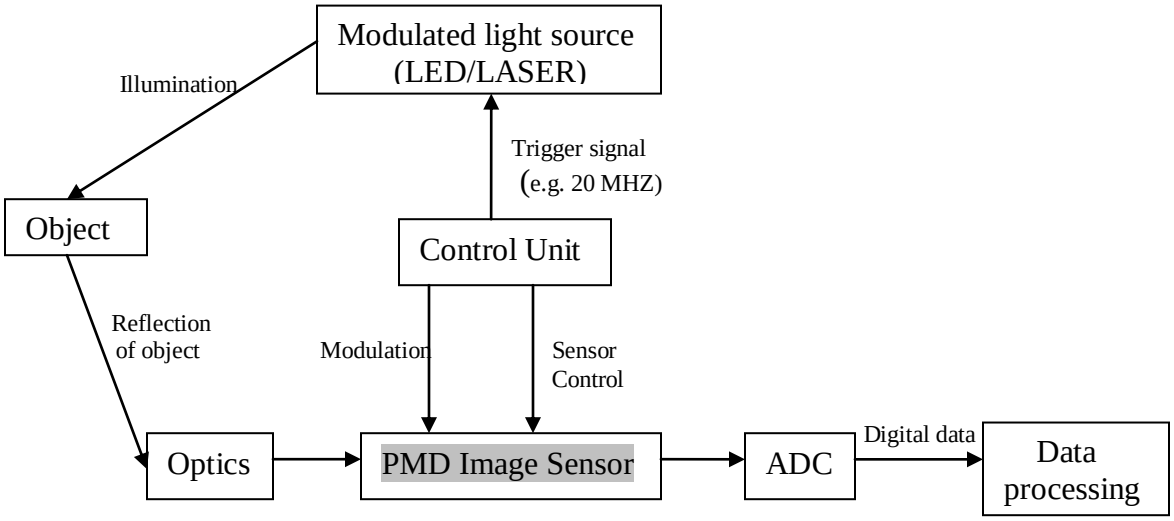

Figure 1: Block diagram of 3D TOF camera

The block diagram of 3D camera is show above in fig: 1. The main components in the camera are PMD image sensor and modulated light source. The Light Emitting Diode (LED) transmits the modulated light. The control unit sends the signal to LED to emit the modulated light. The modulation frequency can be changed from minimum of 0HZ to 80MHZ based on the scenario.

The normal modulation frequency is 20MHZ and it could illuminate the objects up to a distance of 7.5m (f = 20 MHZ, ʎ=15m, d= ʎ/2). The active light should reach the sensor after the reflection from the object, the illuminated light travels twice the distance (d). The imaging Time of Flight measurement based on PMD sensor is shown in fig: 2.

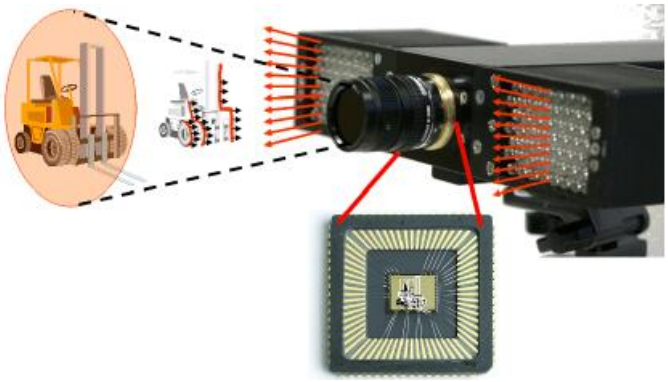

Figure 2: Imaging Time of Flight measurement based on PMD. [*Thorsten*]

The quality of the 3D image depends on the amount of active light which is received by the PMD imager. The illuminated light which reaches the imager has phase shift after the reflection from the target. The control unit is configured to produce four samples of picture (A1, A2, A3, and A4) each with phase shift of 90°, which is proportional to distance. By acquiring the complete four images sequentially in the pixels, each pixel of the imager calculate the distance to the target (phase), grayscale value of the target (amplitude). Higher the amplitude, the more precise the distance calculation. The phase, strength of the signal (amplitude), gray scale value, and the distance equation are shown in following.

Phase calculation => $\varphi =$ $\arctan\left(\frac{A_1 - A_3}{A_2 - A_4}\right)$ (Eq: 1)

Strength of the received signal (amplitude) => $a = \sqrt{\frac{(A_1 - A_3)^2 + (A_2 - A_4)^2}{2}}$ (Eq: 2)

Grey scale value of each pixel => $b = \frac{A_1 + A_2 + A_3 + A_4}{4}$ (Eq: 3)

Distance to the target => $d = \frac{c.\varphi}{4\pi.f_{mod}}$ (Eq: 4)

The fig: 3 show the signal received by PMD sensor. The black wave in the fig: 3 is the modulated light from LED (emitted light) and four red bars are the samples of the image after the reflection of the light on the target (reflected light). By using Auto Correlation feature the phase delay (φ) between the emitted waves and reflected wave is identified. The amplitude (a) in the

fig: 3 show quality of the 3d measurement. The gray scale (b) is the intensity (brightness) of the image. The depth and the intensity of the image depend on the illumination, field of view, optics, fill factor and sensor area.

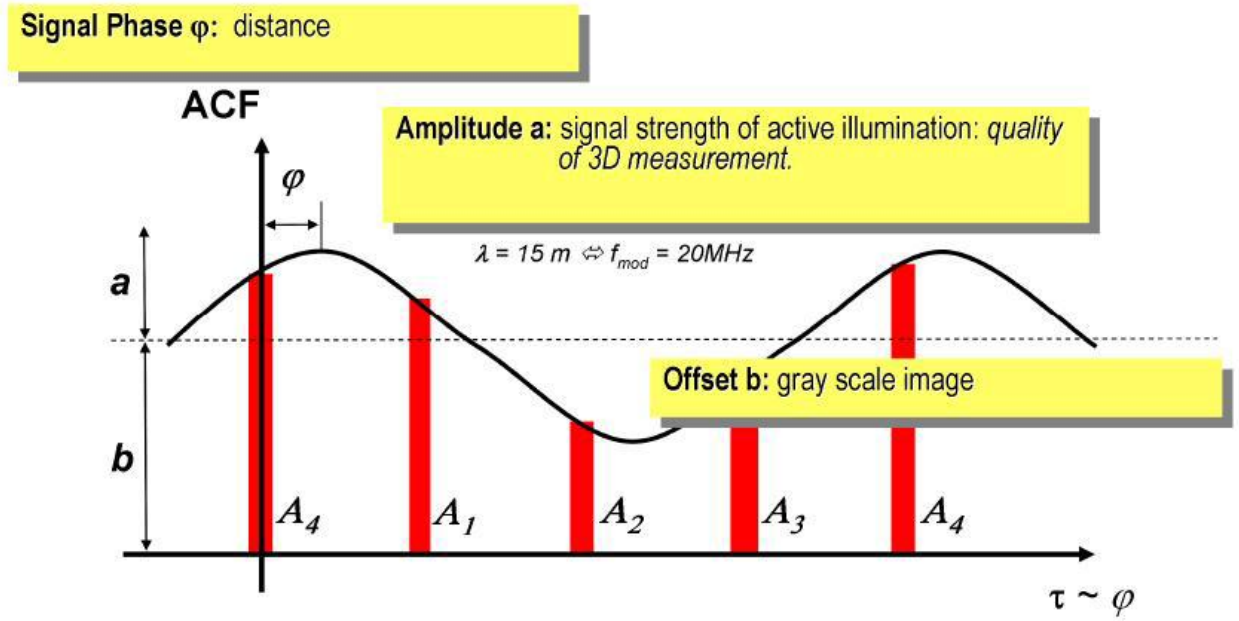

Figure 3 : PMD signal phase, amplitude and offset. [*Thorsten*]

Table 1: Important parameters of photon ICs 19k-S3 image sensor

Sensor Area	7.2mm(H) × 5,4 mm (V)
Modulation frequency	Min. - 0HZ, Typ.-20MHZ, Max.-80MHZ
Fill factor	40%
Size of pixel	45µm (H) × 45µm (V)
Quantum efficiency @ 1MHZ	50%
Quantum efficiency @ 20MHZ	40%
Conversion gain	4.5 µV/e
Dark current	150fA
Read out	Progressive scan with ROI Global shutter Global reset

2.2 Radiation Sources

The charged particles are of various types and generated by different sources, it can be classified as trapped and transient. The trapped charged particles are present in the magnetosphere, these particles are spread around the earth surface at various altitude. The transient particle events occur based on the solar activity. It is listed in the following table: 1

Table 2: Charged particles from various sources

Charged Particles from various sources		
(Trapped) Particles in Van Allen belt. (i) Protons (ii) Electrons (iii) Heavy Ions	(Transient) Solar Particle Events (i) Protons (ii) Heavy Ions (iii) Electrons	(Transient) Galactic Cosmic Radiation. (i) Protons (ii) Heavy Ions (iii) alpha

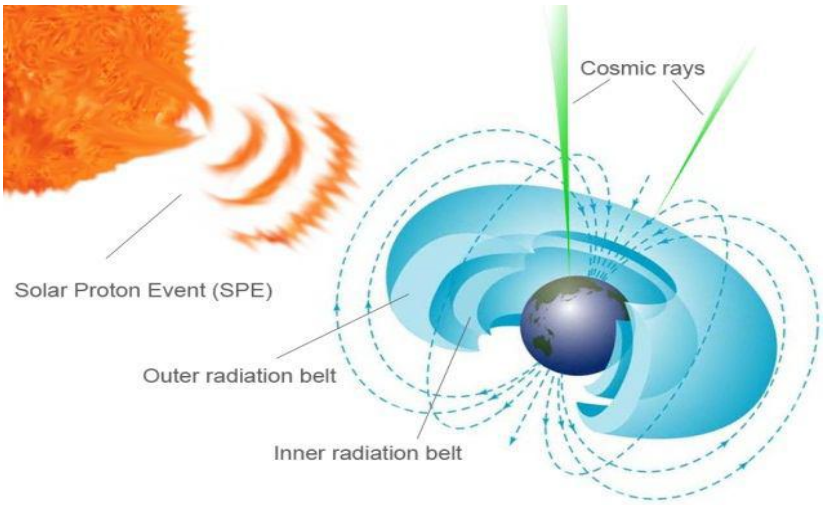

Figure 4: Sources of the space radiation. [*Sakovsky*]

2.2.1 Trapped particles in Van Allen belt

The Van Allen belt is formed in the earth magnetic field (magnetosphere). The solar wind is the source for the radiation belt. The radiation belt mainly consists of electron, proton and heavy ion. The radiation belt is divided into two zones, inner belt and outer belt. The inner belt starts between 300 to 1000 km and lasts until 10000 km. The outer belt starts at 10000 km and spreads beyond 36000 km. Flux is the rate at which particles impinge on an unit surface area (particles/cm^2-s). The fluence is the number of particles that impinge on an unit surface area (particles/cm^2). The trapped proton and electron population varies according to the altitude.

The proton above 10 MeV lies in the altitude below 2000 km. In the low altitudes at south Atlantic the flux of protons with energy greater than 30 MeV is higher (10^4 times) than the other regions of earth. The lower energy proton less than 1.0 MeV spreads over wide region until geosynchronous altitude. The typical satellite shielding can protect it from the protons with energy below 10 MeV. The trapped electron with maximum energy of 7 MeV lies in the outer belt. The inner belt electrons contain maximum energy of 5 MeV. The table: 2 contain the proton fluence at various altitude and orbital inclination. [*L.D. Edmonds*] [*Sanchez*] [*Lima*] [*James*]

Table 3: Annual proton fluence. [*G.M. Swift*] [*Johnston*]

Mission	Proton Fluence (particles/cm^2)
LEO (60º, 300 km) 60 mills Al shielding	6×10^8
LEO (28º, 600 km) 100 mills Al shielding	2.4×10^9
LEO (98º, 705 km) i) 100 mills Al shielding ii) 60 mills Al shielding	 8×10^9 3.6×10^9

2.2.2 Solar Particle events

The solar flares and coronal mass ejection events occur in the sun. It ejects electron, proton, heavy ions and alpha particles. In solar flares (90-95%) the emitted particles are protons. Heavy ions constitute only small per cent of the emitted particles. The electrons from solar eruption have low energy. The protons from solar flares sustain for few hours to few days and it has energy till 100 MeV. Contribution of heavy ions is less when compared to heavy ions form the cosmic radiation. The solar events are patterned base on the eleven year solar cycle. The high fluence of proton event occurs most in solar maximum. [L.D. Edmonds] [James] [Lima] [Sanchez]

2.2.3 Galactic Cosmic Radiation

The GCR originates from outside the solar system. During solar minimum the exposure of GCR is more. The Galactic cosmic radiation contains about 85% protons and 14% alpha particles and 1% heavier nuclei. Comparing the solar eruption and radiation belt protons, the effect of GCR is less in equator and more in poles due to less geomagnetic shielding. It has low flux (particles/cm^2-s) but high energy. The GCR mainly considered for SEE (Single Event Effects) in electronics. The main source for the radiation effects in electronics on orbit is due to proton and electron in Van Allen belt. The second cause is due to solar protons and third source is GCR heavy ions. The table: 3 contain the source of radiation in LEO, for the orbit inclination less than and greater than 60° and respective radiation effects. [*James*] [*Lima*] [*Sanchez*]

Table 4: Source of radiation at different orbit inclination. [Lightsey]

Space hazard	Single-Event Effects			Total Ionizing Dose	
Specific Cause	Cosmic Rays	Trapped radiation	Solar particle	Trapped radiation	Solar Particle
LEO <60º	Relevant	Important	Not applicable	Important	Relevant
LEO >60º	Important	Important	Important	Important	Relevant

The flux of these sources is affected by the activity of the solar cycle. The solar cycle contain two phases, the solar minimum and solar maximum. The duration of the solar cycle is eleven year, four years of solar minimum and seven years of solar maximum. The fluence, flux and energy of the particle vary based on the altitude and inclination of the orbit. The table: 4 below summarize the list of charged particle, its variation during solar cycle and its effects on respective orbits.

Table 5: Variation in the flux of the charged particle during the solar cycle. [*Lima*]

Particle type	Solar cycle & variation in flux	Types of orbit affected
Trapped – Protons	Solar Min - Higher Solar Max – Lower	LEO, HEO, Transfer orbits.
Trapped – Electrons	Solar Min – Lower Solar Max – Higher	LEO, GEO, HEO, Transfer orbits.
Transient - GCR ions	Solar Min – Higher Solar Max – Lower	LEO, GEO, HEO.
Transient - Solar protons	During Solar Max only	LEO (I>45º), GEO, HEO.
Transient - Heavy ions	During Solar Max only	LEO, GEO, HEO, Interplanetary.

2.3 Effects of radiation

The charged particle in space affects the electronic in the orbit. It causes various effects in electrical and electronics system in satellite. The radiation effects are broadly classified into two types, cumulative effects and Single Event Effects (SEEs). The various effects of radiation are classified in the fig: 2.

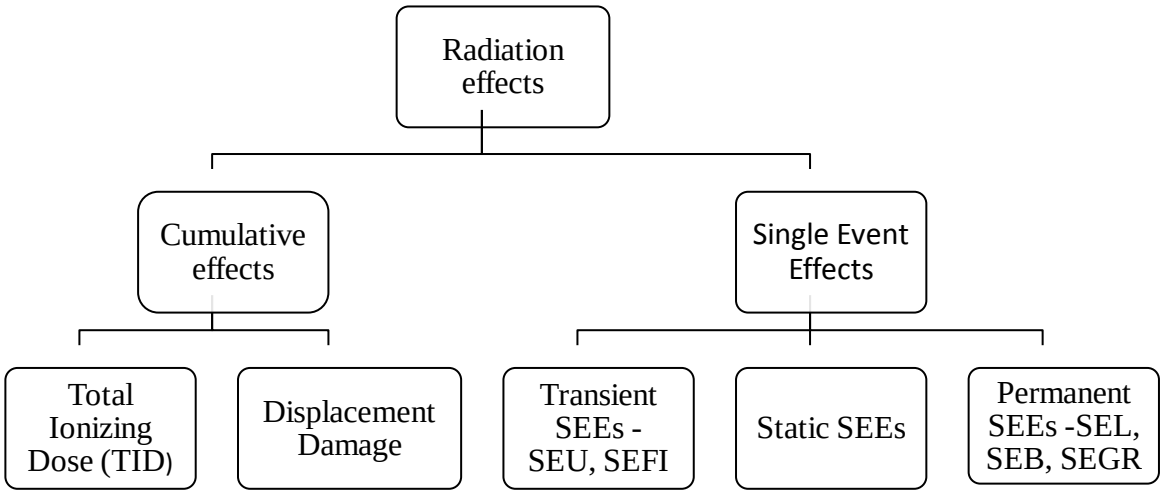

Figure 5: Classification of radiation effects. [*Faccio*]

2.3.1 Cumulative effects

The cumulative effects are due to microscopic defects in the component. These small defects do not affect the performance of the component. But over period of time these minor defects cause measurable effects and even cause failure of the components. It is classified into two types, Total Ionizing Dose (TID) and Displacement Damage (DD).

(i) Total Ionizing Dose:

The electron, proton and heavy ions from the radiation sources cause ionization, when they incident on the matter (semi-conductor). It generates electron-hole pair. The ionizing particles loss their energy when they travel through the matter and that energy is deposited in the matter. Energy loss of the particle is classified into two types; they are electronic energy loss and nuclear energy loss. The interaction of electron of the atom deals with electronic energy loss and interaction of nucleus of the atom deals with nuclear energy loss. The TID causes only electronic energy losses. The measure of total energy deposited per unit mass of the material through ionization is defined as Total Ionizing dose (TID). TID is measured over period of time, the effect of ionization increases gradually over the mission duration. The TID is measured in Gray (GY) in SI system, but traditionally the total dose is measured in rads (1GY = 100 rad).

The effects on CCDs are increased dark currents, effects on MOS transistor (Threshold voltage of the MOS transistor would shift) and Charge Transfer Efficiency. In CMOS sensor the effects are changes to MOS-based circuitry of imager, including change in pixel amplifier gain. Power consumption of the digital circuit would change. High leakage current cease the functionality of the circuit and it would lead circuit failure. [*Edmonds*] **[***Faccio*] [*Lima*] [*Swift*] [*Richard*] [*ESA2010*] The technologies susceptible to TID effects are give in the table: 21.

(ii) Displacement Damage:

The radiative particles traverse the crystalline material, displaces the atoms from the normal lattice sites and it deforms the material structure, by non-ionizing energy losses. It is known as displacement damage effect. This effect depends on incident particle type, incident particle energy, particle fluence (particle/cm^2) of the surrounding and the incident material. The displacement damage effect is estimated using NIEL (non-ionizing energy loss). In DD the material does not loose energy by ionization but by elastic/inelastic collision with nuclei in the material. This effect is more important for photo detector and electro-optic integrated circuit.

The effects on CCD and CMOS image sensor are increase in dark current, reducing gain and charge transfer efficiency (CTE) , increases hot spots(bad pixel flagged by software), Random Telegraph Signal and less responsivity. The effect on LEDs is reduced light power output. The proton testing is used to measure the displacement damage effect of the material. The proton testing is done using proton with energy between 10 to 200 MeV. There are possibilities in which high energy electron could cause displacement effect. In that case electron testing with energy of 3 MeV or higher can be done. **[***Faccio*] **[***Lima*] [*Swift*] [*Richard*] [*ESA2008*] Summary of displacement damage effect as a function of technology of the component is given in table: 22 and definition of DD effects are shown in table: 23.

2.3.2 Single Event Effects (SEEs)

The Single Event Effect is caused when a single charged particle pass through the device and losses their energy by ionizing the device. It deposits enough energy on the matter to cause a failure in a single strike. It might also cause nuclear interaction with the incident material. These are transient effects. The SEEs can be destructive or nondestructive. If the device fails then it's destructive and if the device losses data or control then it is nondestructive. The SEE of the device is estimated by two parameters, Q_{crit} and L.E.T. The Q_{crit} is minimum amount of charge required to cause a soft error at any given node, it is measured in pico coulomb (pC). The silicon requires 22.5MeV of energy to generate 1 pC of charge (22.5 MeV is the stopping energy of silicon). When the deposited energy is higher than its stopping energy of the material, then it generates the charges at nodes. If the charge generated is higher than Q_{crit} then an SEE occurs in the device. When Q_{crit} for a device is increased then it's SEE rate is decreased. **[***Faccio*] **[***Lima*] [*Richard*]

The sensitivity of the device to SEE is characterized by LET versus cross section, it is shown in fig: 3. The amount of energy transferred during ionization is given by Linear Energy Transfer (LET) function. It is measured in MeV.cm^2/g or KeV/µm. LET threshold is the minimum LET to cause an effect. The L.E.T varies depending on incident particle mass, incident energy and angle of incidence. The number of upset or errors, divided by number of particle per cm^2 (fluence) is referred as cross section (σ). The saturation limit (σ_{lim}) is the cross section of the sensitive area. By the following four weibull parameters, LET threshold (LETth), saturation limit (σ_{lim}), width (W) and Power (S). SEU rates for a device can be generated by spenvis radiation model software. The upset or error rate are represented in, per bit, bit per second, and bit per day. SEEs test can be performed in a particle accelerator. Mainly there are three types of SEEs, transient, static and permanent Single Event Effects. It is explained in following. **[***Faccio*] **[***Lima*] [*Johnston*]

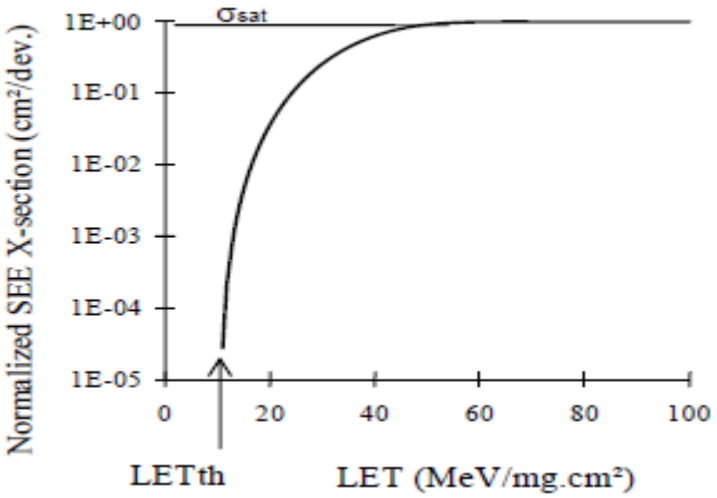

Figure 6: LET versus cross section curve. [*ESA2010*]

(i) Permanent SEEs:

These effects cause permanent damage or failure. Single Event Latchup (SEL), Single Event Burnout (SEB), Single Event Gate Rupture (SEGR) are categorized under permanent SEEs. SEL occurs in CMOS technologies. The sustained high-current state induced by a single-particle interaction is referred to as single-event latch-up (SEL). The Latchup increase the current, if the power supply is maintained then the device is destroyed by thermal effect. By monitoring the current and power control circuit the damage can avoided. Single Event Burnout (SEB) occurs in power MOSFETs; the power devices are sensitive to SEB, when the device is in a biased off state. It's similar to SEL. The permanent damage of the device occur when short-circuit current induced across the high voltage junction. Single Event Gate Rupture (SEGR) also affects power MOSFET in the 'off' state. The incident particle forms a conduction path in a gate oxide, resulting in device damage. **[***Faccio*] **[***Richard*]

(ii) Static and Transient SEEs:

This effects does not cause any permanent damage or failure, it cause errors (bits of information stored in logic circuit or in a storage device is changed) when the incident material is ionized. This effect is known as Single Event Upset (SEU). Static Random Access Memory (SRAM) and Dynamic Random Access Memory (DRAM) and other memory devices are affected by the SEU. By resetting, the device is operational. The Single Event Functional Interrupt (SEFI) is caused by ion strike; it leads to temporary non-functionality of the affected device. The transient SEEs cause variation in the amplitude of the signal. This effect is notable in most of the device. It mostly occurs in linear regulators and converters. The radiation effects due to different charged particles are summarized in the table: 5 and possible single event effect as a function of technology of the component is given in the table: 24. **[***Faccio*] [*Johnston*]

Table 6: Radiation effects of different particle. [*Lima*]

Particle origin	Particle	Effects
Trapped	Protons	Total Dose SEEs Displacement Damage Solar cell degradation
	Electrons	Total Dose Solar cell degradation
	Heavy Ions	SEEs Dose exposure for humans
Transient	Solar Protons	Total Dose SEEs Displacement Damage Solar cell degradation
	Solar Heavy Ions	SEEs
	Galactic Cosmic Rays	SEEs Dose Exposure for humans

In the above listed SEE, the permanent effects are caused by the solar heavy ions and GCR particles. The probabilities of heavy ions are higher in solar minimum cycle. But there are no exact number of events and possibility of occurrence of permanent failures on components. In CMOS technology the most common failure is SEL. The transient SEEs can be estimated by SPENVIS software. The SEU for a device over a day is estimated. The SEU rate (per bit per day) varies for each device based on three functions. They are design and manufacturing technology, LET threshold, and maximum sensitive surface of the component. The following are the range of upset rates of the components.

i) Bipolar - 1.91E-02 to 4.92E+00 errors/bit-day
ii) CMOS - 3.34E-05 to 5.43E-02 errors /bit-day
iii) RAM - 5.65E-05 to 4.92E-03 errors/bit-day
iv) SOI - 2.81E-05 errors/bit-day

At the initial stage of the testing, the most important radiation effects for image sensor are TID and Displacement Damage. But in this thesis only TID are considered for the testing due to the factor of time and cost of testing. The radiation sources which are explained in the previous chapter are considered for the implementation of radiation testing. In the later chapters only TID is discussed for the design and implementation of radiation testing. Next section deals with the orbital experience (previous mission information's) of the electronics in exposing to radiation. The total amount of dose (rad) absorbed by the device over a period of time in the target orbit is discussed in the next chapter.

2.4 Orbital experience

The primary idea of this paper is to test the radiation tolerance of the PMD PhotonICs 19k-S3 image sensor (3D chip). The image sensor is based on the CMOS technology. This 3D image sensor is planned to use for satellite operation. The radiation tolerance of the component is based on the design and manufacturing technology of the component. The COTS components are not designed in such way to withstand the radiation. In order to confirm the operation of the image sensor in the orbit, the respective sensor has to be tested for radiation tolerance.

The COTS components manufactured under various technologies like cmos, mos, rmos, fpga, bipolar, dram, sram, soi, sos, epi. Each of this technology reacts differently to the radiation and their effects differ. The radiation testing and parameter measurements should be designed based on the technology of the component. In general the COTS components have radiation tolerance of 1 – 10 Krad/year [*JSC*] and untested COTS component (Si) is estimated to have radiation tolerance up to 5 Krad [*Underwood*]. The radiation tolerance (dose) of PMD image sensor is unknown because it has not been tested in radiation. Hence the total dose requirement for the respective orbit is estimated using spenvis and from data's of the previous mission. The table: 6 show the required total dose for various orbits. The component is shielded by Aluminum with thickness of 100 mills (2.54 mm).

Table 7: Total Dose requirements for respective space mission. [*Kayali*]

Description	Orbit	Operating time (years)	Total Dose (rad) (SiO_2)
Space station	500 km, 54º	10	5×10^3
High inclination earth orbiter	705 km, 98º	5	2×10^4
Geostationary	36,000 km	5	5×10^4
Mars surface exploration	NA	3	10^4
Mission near Jupiter	NA	9	1.5×10^5 - 2×10^6

Table 8: One year dose at center of solid (Al) sphere at ISS. [*ISS*]

Shielding (MILS)	Shielding (MM)	Shielding (G/CM^2)	Trapped Electrons (rad)	Trapped Protons (rad)	Total Dose (rad)
3.000E–02	7.620E–04	2.118E–04	9.016E+05	9.762E+04	9.922E+05
5.000E+01	1.270E+00	3.531E–01	1.939E+03	9.013E+01	2.029E+03
8.000E+01	2.032E+00	5.649E–01	9.355E+02	7.658E+01	1.012E+03

The orbit of our mission is LEO polar orbit. Apogee is 600 km and Perigee is 400 km and inclination of 89º. In the table: 6 the high inclination orbiter were quiet close to our mission orbit. According to the high inclination earth orbit in (table: 6) with shielding of 100 mills (2.54 mm), the total dose of (SiO_2) for one year is 4 Krad. This could be the closer approximation to our orbit. The 4 Krad is within our specified limit of dose of (1-10 Krad). The table: 7 contain the total dose absorbed for various shielding thickness at the ISS orbit over one year. The altitude of ISS is apogee-437 km and perigee-361 km. This altitude is quiet close to our orbit, but the inclination of the ISS orbit is 51.59º which is entirely different scenario in comparing to our orbit inclination. From the (table: 6) it is evident that, at ISS orbit the total dose acquired for one year is (1.012 Krad) for a shielding of 2 mm thickness is closer to our results generated in spenvis. The results from spenvis are discussed in the next chapter.

In an another reference, the Sony XC-ST70CE camera is used for stereo vision measurement in LEO orbit with shielding of 3mm thickness and for a duration of one year. It's irradiated up to 3 Krad to test its performance [Rerrario]. The Commercial sensor survey testing report was made by NASA. In that CMOS based "Micron 5MPX" and "Micron 3MPX" was tested for radiation tolerance. The cameras tested for TID from 0.5 Krad to 5 Krad. [*Becker*]

By comparing the data of the previous testing and mission, also by considering the shielding constraints and safety of the device, the image sensor in our mission should be irradiated up to 5Krad in radiation test facility to ensure its radiation tolerance for our mission. In this chapter, radiation sources, effects, and total dose exposure in orbit is discussed and amount of dose the device should withstand in orbit is estimated from the review of various papers. In the next chapter, the total dose exposed in the target orbit is estimated using radiation model software (SPENVIS) is discussed. The theoretical and simulated solution is compared to find the balanced total dose exposure value for the irradiation at radiation testing facility.

3. Spenvis radiation model

The Space Environment Information System (SPENVIS) is ESA operational software. It is developed and maintained at Belgian Institute of Space Aeronomy since 1996. It's a World Wide Web tool and it provides information on the space environment and its likely effect on space systems. In SPENVIS spacecraft trajectory or coordinate grid is generated. The flux and fluence of the charged particle around the trajectory is estimated. By estimating the radiation sources, TID, DD, and SEEs for simple geometry is calculated. The information provided by this software is acquired from the earlier space mission's data.

Spenvis is used for estimating the various effects of radiation for electronics on orbit. For this mission spenvis is used for estimating the Total Ionizing Dose (TID) for silicon (Si). It is radiation model software; the first step is the input of spacecraft trajectories and mission duration. The altitude and inclination of the orbit is perigee = 400 km, apogee = 600 km, inclination = 90º. Estimation is made for mission duration of 3, 6, and 12 months. Next, radiation source has to be defined for this model. In this radiation model we have to test the Total Ionizing Dose effects. In order to measure this effect on silicon (Si), the sources of radiation have to be defined. The radiation sources are selected and their properties are defined.
The defined radiation sources in spenvis are;

(i) Trapped particles radiation model
(ii) Long- term solar particles fluences
(iii) Galactic cosmic ray fluxes

3.1 Trapped particles radiation model

The trapped particle flux model has three different proton and electron modules. The AP-9 proton model and AE-9 electron model is selected for this mission. The AP-8 and AE-8 model cover the full spatial and spectral range of the radiation belts. The AP-8 has the energy range from (0.1 MeV to 400 MeV), and the coordinate range (L) from 1.14 to 6.6 (L=1=Earth radius). The AE-8 has the energy range from (0.04 to 7MeV) and coordinate range from (1.14 to 12). The AP-8 and AE-8 model have the option to select between solar cycle of maximum and minimum. The solar cycle of maximum is selected for the trapped particles. [*SpenvisT*]

Using the specified orbital parameters and AP-9, AE-9 radiation models, the average spectra of trapped electron and proton for the respective orbit is estimated. The graph in fig: 3 and fig: 4 show the average spectra of trapped electron and proton for one year. The graph shows the integral flux and differential flux in vertical axis and energy of the proton in horizontal axis. The integral flux represents the number of particle (fluence) of given energy in the orbit per unit area and unit time. The differential flux is the number of particles (fluence) per unit area, unit time and unit energy. The energy range in the horizontal axis is from 0.1 to 1000 MeV. The proton with maximum energy in the orbit is 300 MeV and minimum energy is 0.1 MeV. The graph shows that the flux of the trapped proton in the orbit decreases gradually as the energy of the

trapped proton increases. Number of protons (fluence) decreases gradually as the energy of proton increases. The flux and fluence for the trapped protons, energy range from 0.1 to 300 MeV is given in the table: 15

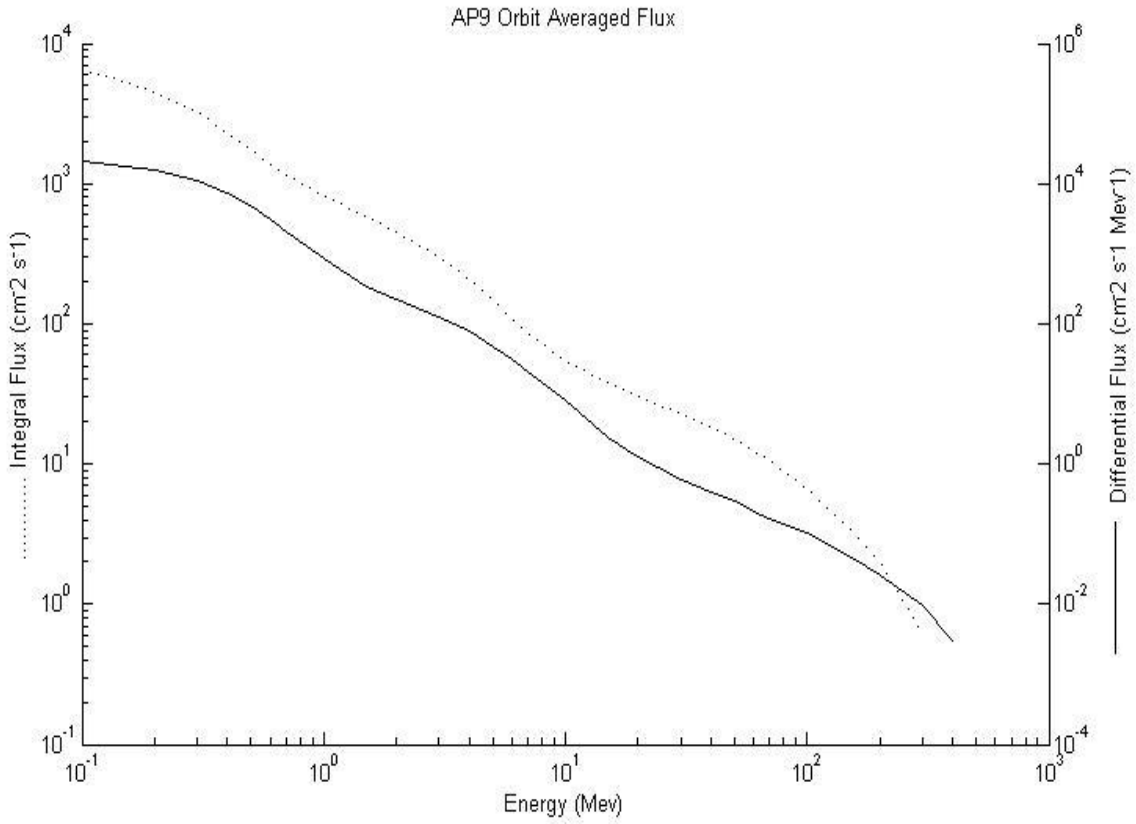

Figure 7: Average spectra of trapped protons for one year

The Figure.4 below shows the average spectra of trapped electron. The energy range of trapped electron in the orbit is 0 to 10 MeV. The electron with maximum energy in the orbit is 7MeV. The graph shows that the flux of the trapped electrons in the orbit decreases gradually as the energy of the electron increases. Number of trapped electrons (fluence) decreases gradually as the energy of electron increases. The flux and fluence for the trapped electrons, energy range from 0.04 to 7 MeV is given in the table: 17

The satellites in LEO with higher inclination between 45to 85 deg have increased number of electron in both northern and southern hemisphere [*JSC*]. The total mission fluence of trapped particle in the orbit is calculated by sum of all values in different energy ranges of integral spectra. The fluence is calculated without shielding. The total number of electron encountered by the detector in the orbit, in one year is 1.98E+13 (particles/cm^2).

The total number of proton encountered by the detector in the orbit, in one year is 9.12E+11(particles/cm^2). Hence the number of trapped electrons in the target orbit is higher than the number of trapped protons.

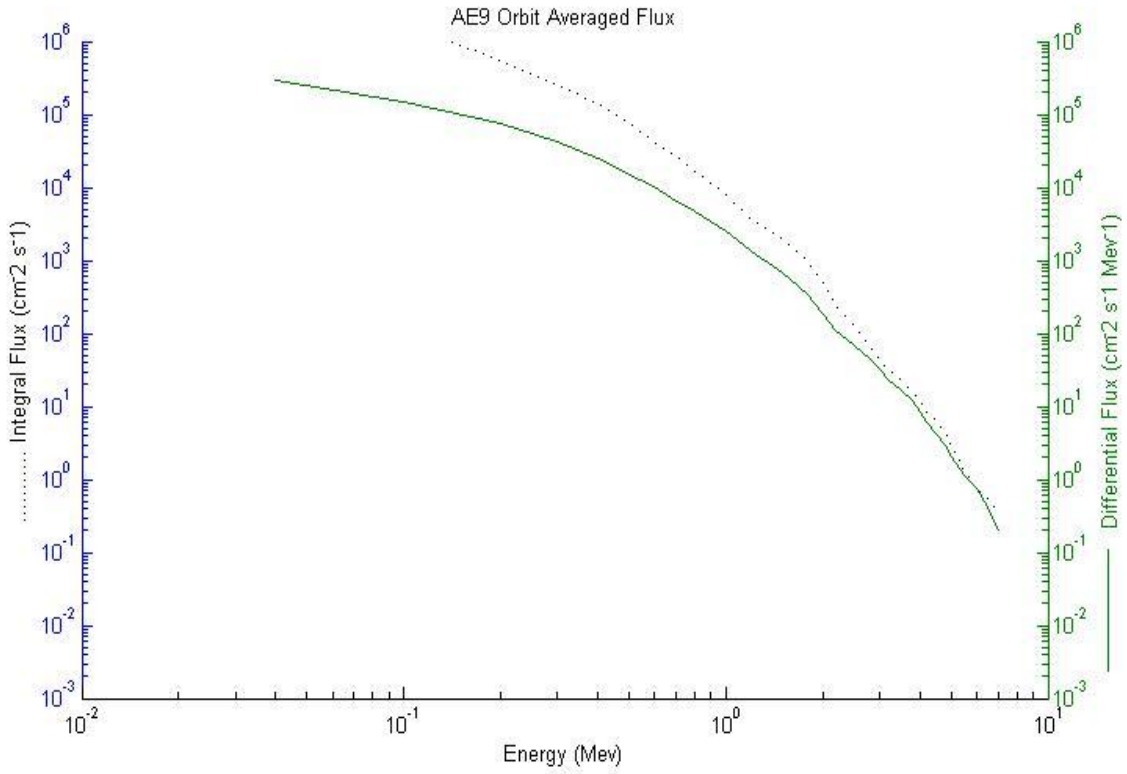

Figure8: Average spectra of trapped electrons for one year

The fig.5 & 6 shows the distribution of proton and electron at an altitude of 400 to 600 km in the world map. The proton is distributed over in particular region from -10º to -80º latitude and -60º to 60º longitude and -15º to -80º latitude. The most of proton is present over south atlantic, this is due to the south atlantic anomaly. The trapped electrons are more widely distributed over the earth than the protons. The electrons are densely populated in both northern and southern hemisphere. The satellite with higher inclination encounters more electron than proton. The electrons are located over 45º to 75º N and -15º to -90º S latitude. In the longitude it's spread over -180º to 180º. In the following table:1 Integral spectra of the trapped proton and trapped electron are listed.

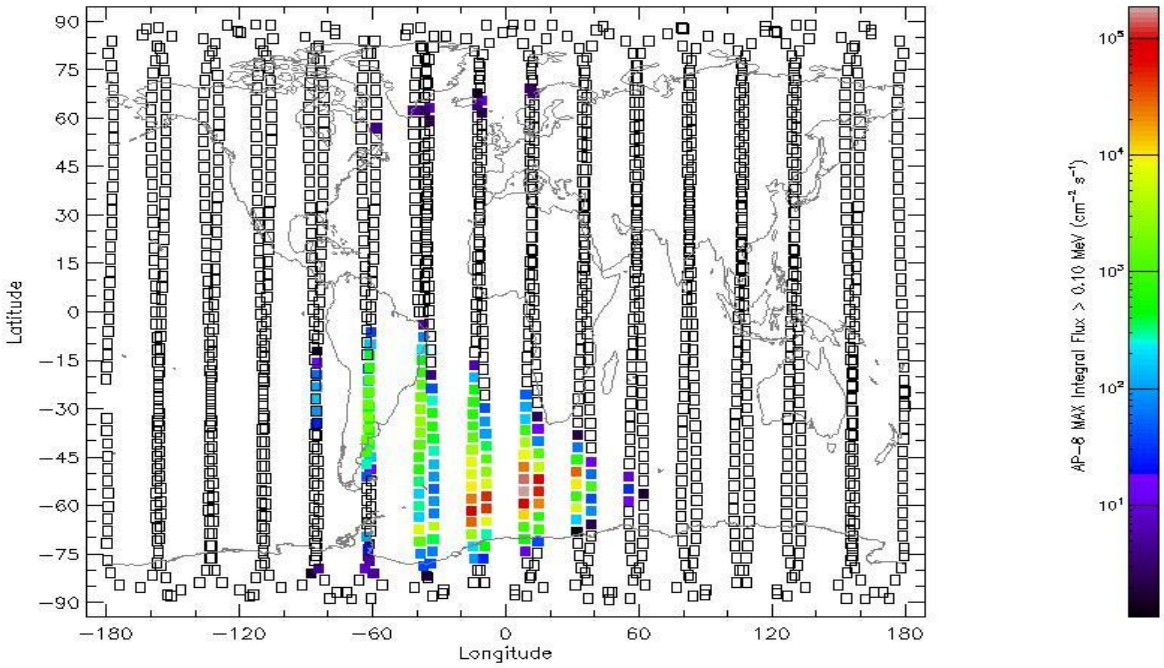

Figure 9: Trapped proton flux distribution at an altitude of 400 to 600 km

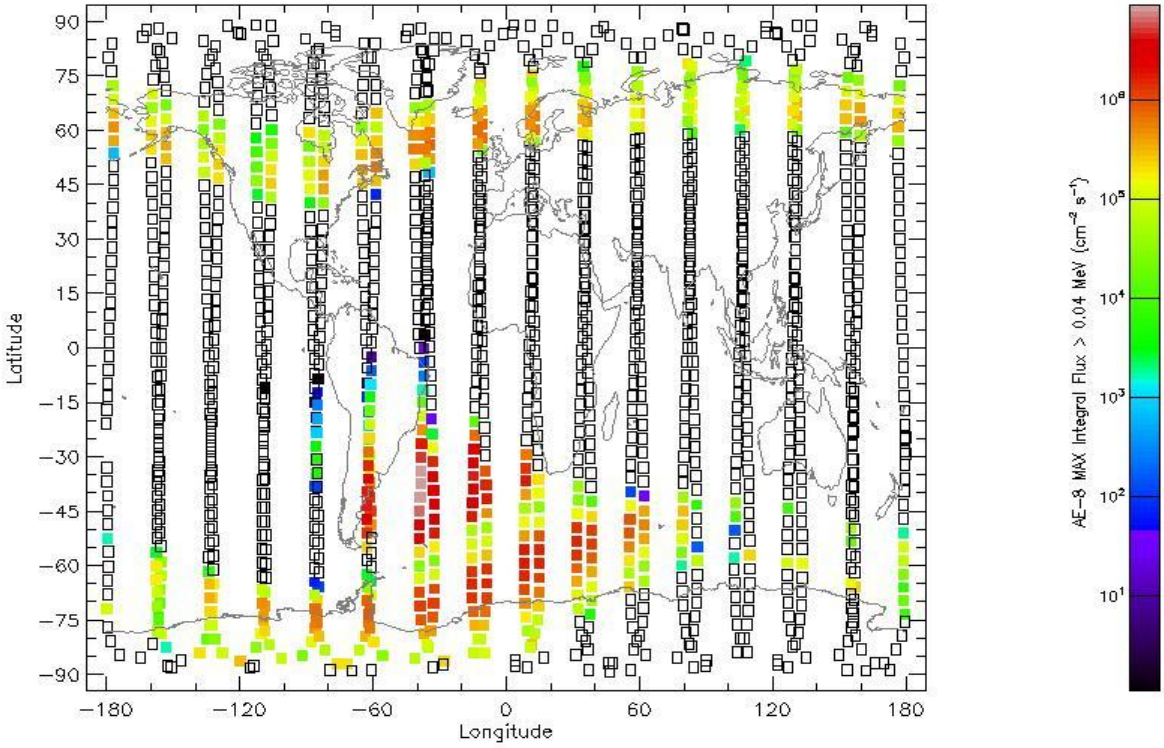

Figure 10: Trapped electron flux distribution at an altitude of 400 to 600 km.

3.2 Long term solar particle fluences

The Long-term solar particles fluences model have the inputs from solar particles. The worst-case scenario module is selected for the solar particle fluence. The solar maximum is chosen. The long term solar particles fluence model contains two types of particle, solar protons and solar ions. The ESP model is used to predict the average flux and fluence of the solar proton. The ESP model contains the data's of three different solar cycle and the respective energy levels. The Psychic model is clubbed with ESP model to predict the average flux and fluence of heavy ions. The psychic model contains the differential energy spectra for five of the major elements protons, alphas, Mg, Fe, and elements with atomic number greater than 28. The ion range is selected from hydrogen (H) to uranium (U). The confidence level is 95%. The confidence level is the probability (in %) that the predicted proton fluence will not be exceeded. The magnetic shielding around the earth is enabled in this model. [*SpenvisS*]

The graph below is the plot for the energy of solar protons in horizontal column and integral fluence (number of solar protons per unit area) and differential fluence (number of solar protons per unit area and per unit energy) in vertical column. In the orbit the solar protons has a maximum energy of 500 MeV. In table: 19 contain the total mission solar proton fluence at spacecraft. The table contains the energy, integral and differential solar proton spectrum.

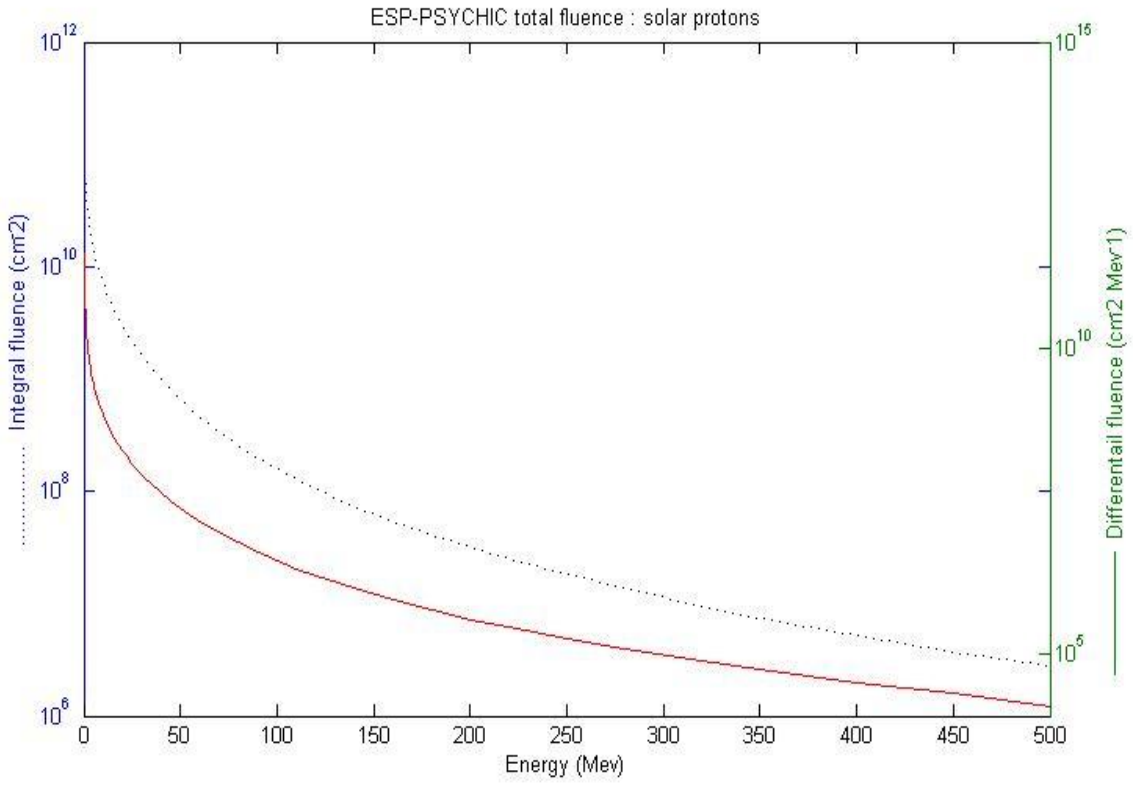

Figure 11: Solar proton fluence spectrum.

The solar ion events occur in solar maximum period. It has higher flux than the GCR. The large events occur in long span of time, for total mission of one year, its complex to predict. The solar ions have maximum energy of 500 MeV.

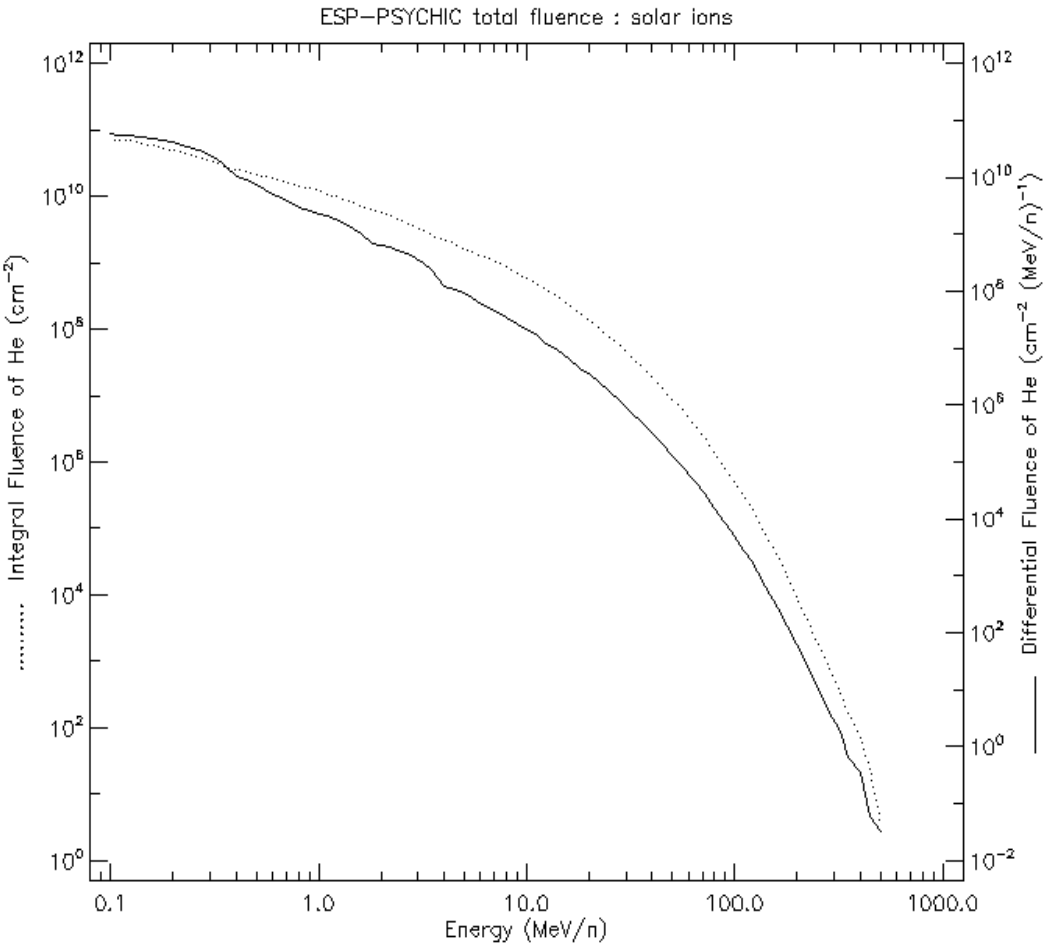

Figure 12: Solar ion spectrum.

3.3 Galactic Cosmic ray flux:

The Galactic Cosmic Ray flux model, have the inputs from cosmic particles. The GCR particles are from outside the solar system. The flux of the particle is changed in relation to the solar activity. Geomagnetic field provides the shielding to GCR particles. Also orbit with higher inclination is susceptible to GCR particles. But still GCR of high energetic particle can cause damage in satellite. The ISO 15390 model and solar minimum is selected. GCR flux is more in solar minimum. The Ion range for GCR is from hydrogen (H) to uranium (U). The table:20 contains the GCR energy range, total mission integral flux, total mission differential flux. The GCR has maximum energy of 20000 (MeV/n). [*SpenvisG*]

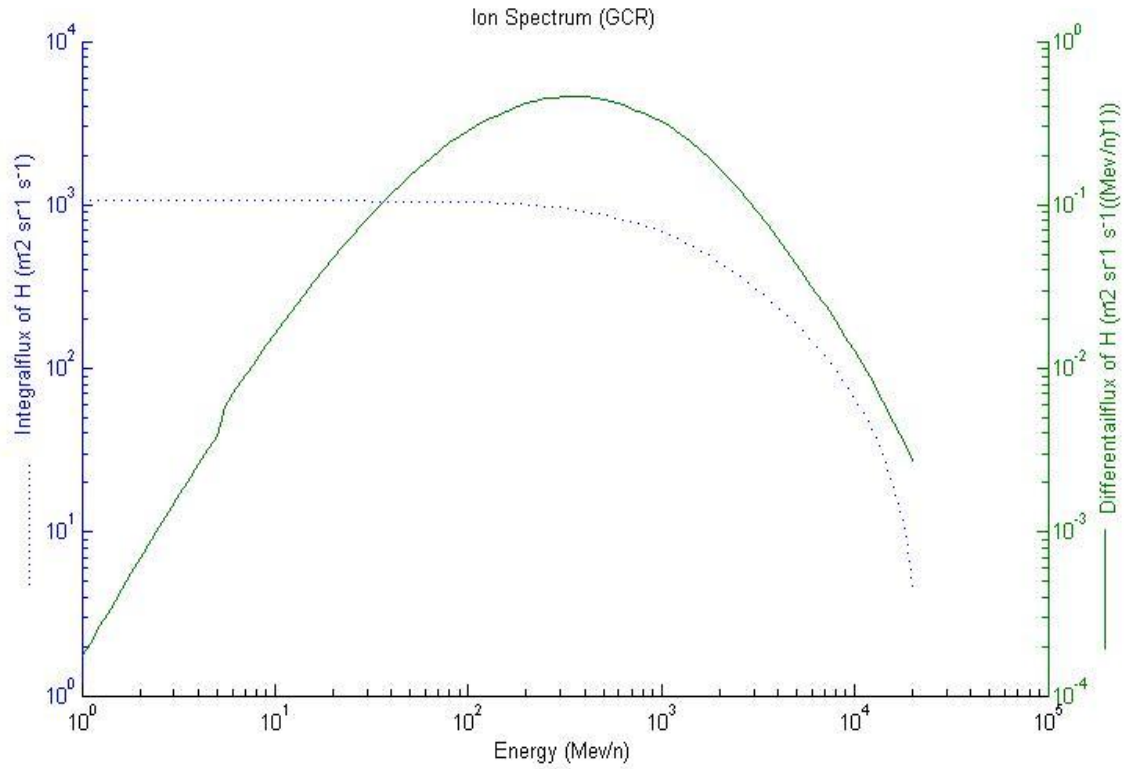

Figure 13: GCR ion spectrum

3.4 Radiation model results

The source of radiation for measuring TID is trapped proton and electron, long- term solar particles fluences. The TID is estimated using Ionizing dose for simple geometries model from spenvis. The shielddose-2 model is used for shielding geometry. The inputs are shielding thickness, shielding material, shielding geometry and target material. The target material is silicon. The shielding material is Aluminum. The shielding geometry is "center of Al sphere". The source of radiation is isotropic. The target material is analyzed with various shielding thickness of (Al) form 10^{-4}mm to 3mm to find out the corresponding total dose.

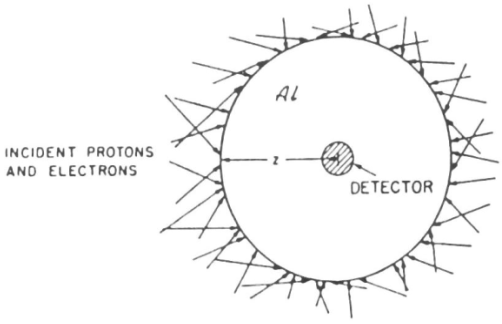

Figure 14: Centre of (Al) sphere

The fig: 11 show the shielding geometry (Centre of sphere) chosen for the radiation model. This geometry is used where the components shielded to a finite level over all finite angles. It is used. It's a function of radius of the sphere. The irradiation is from all directions. [SpenvisD] [SpenvisD2]

Table 9: 1 year - Total mission dose (rad)

Al absorber thickness			Total Ionizing Dose	Trapped Electrons	Bremss-trahlung	Trapped protons	Solar protons	Tr.el.+ Bremss	Tr.el.+Br. +Tr.Pr.
(mm)	(mils)	(g/cm^2)							
0.000	0.004	6.705	3.04E+06	6.70E+05	4.84E+02	9.87E+05	1.39E+06	6.70E+05	1.65E+06
1.4	55.11	0.378	5.90E+03	3.50E+03	2.41E+01	4.21E+02	1.95E+03	3.52E+03	3.95E+03
2.0	78.74	0.54	3.04E+03	1.40E+03	1.53E+01	3.03E+02	1.31E+03	1.41E+03	1.72E+03
3.0	118.1	0.81	1.39E+03	3.53E+02	9.49E+00	2.14E+02	8.13E+02	3.62E+02	5.77E+02

Table 10: 183 days– Total mission dose (rad)

Al absorber thickness			Total Ionizing Dose	Trapped Electrons	Bremss-trahlung	Trapped protons	Solar protons	Tr.el.+ Bremss	Tr.el.+Br. +Tr.Pr.
(mm)	(mils)	(g/cm^2)							
0.000	0.004	0.000	1.52E+06	3.36E+05	2.42E+02	4.95E+05	6.97E+05	3.36E+05	8.31E+05
0.95	37.40	0.257	5.96E+03	4.09E+03	2.00E+01	3.33E+02	1.51E+03	4.11E+03	4.44E+03
1.000	39.37	0.270	5.38E+03	3.67E+03	1.87E+01	3.02E+02	1.38E+03	3.69E+03	3.99E+03
2.000	78.74	0.54	1.521E+03	7.04E+02	7.69E+00	1.51E+02	6.57E+02	7.11E+02	8.63E+02

Table 11: 31 days – Total mission dose (rad)

Al absorber thickness			Total Ionizing Dose	Trapped Electrons	Bremss-trahlung	Trapped protons	Solar protons	Tr.el.+ Bremss	Tr.el.+Br. +Tr.Pr.
(mm)	(mils)	(g/cm^2)							
0.000	0.004	0.000	2.61E+05	5.83E+04	4.27E+01	8.51E+04	1.81E+05	5.83E+04	1.43E+05
0.360	14.17	0.097	5.95E+03	5.06E+03	1.42E+01	2.00E+02	6.78E+02	5.07E+03	5.27E+03
1.000	39.37	0.27	1.03E+03	7.41E+02	3.84E+00	5.14E+01	2.38E+02	7.45E+02	7.96E+02
2.000	78.74	0.54	2.84E+02	1.44E+02	1.56E+00	2.60E+01	1.12E+02	1.46E+02	1.72E+02

The tables above are the results of Total Ionizing Dose requirement for the target orbit, from the spenvis model. The (table: 8, 9, 10) contain the estimated TID for 1 year, 6 months, and 1 month respectively. Each table contain the Aluminum shielding of various thickness, TID in rad, doses caused due to trapped electron, Bremsstrahlung, trapped protons and solar protons. When electron is deflected by heavy particles then part of the energy (rad) is emitted, it is known as bremsstrahlung.

The first row of the table: 7 contain the TID for a shielding of (10^{-4} mm) 0.004 mils. This is minimum possible shielding thickness available in spenvis for TID calculation. We consider this minimum thickness (10^{-4} mm), as a component without shielding. The component without shielding in the orbit over a period of one year acquires the TID of 1.52×10^{-6} rad. According to the first limitation, the COTS component should not exceed the Total dose of 1-10 Krad/year. By the knowledge of various missions in the similar orbit, this was discussed in the last chapter. The component would able to survive with 5.9 Krad of total dose for duration of one year with a shielding of 1.4 mm. In order to ensure the safety of the mission, the component should be shielded with 2mm thickness of Al. The component with 2mm of shielding in orbit over one year absorb total dose of 3.04 Krad.

The target material silicon (Si) shielded in Al sphere of thickness 2mm contains the following absorbed doses. The table: 8 shows that dose due to trapped electron is the main source of radiation, which produce dose of (1.40E+03 rad). This was discussed in the previous section. The second main source is solar proton, it produce dose of (1.31E+03rad). The trapped proton has the dose of (3.03E+02 rad). The Bremsstrahlung produces the dose of (1.53E+01 rad). The Total mission dose is (3.04E+03 rad). The value of 3.04 Krad is within the criteria of COTs component of 1- 10 Krad. The component without shielding should be irradiated in the radiation test facility up to the total dose of 5Krad. If the component would survive the irradiation without functional failure until 5Krad or at the least until 4.56 Krad (which is 1.5×3.04 Krad, its based RDM) then the component would probably survive in the orbit with shielding of 2mm for one year.

The duration of the mission in the orbit is classified into maximum of one year, minimum of 1 month and in average of 6 months. The total absorbed dose in 6 months with 2mm shielding is 1.5 Krad and for one month it is 0.28 Krad. The Fig.11 shows the dose absorbed by Silicon at the center of Al sphere, for various thicknesses. The graph contains the doses due to electrons, bremesstrahlung, trapped protons, solar protons and total dose.

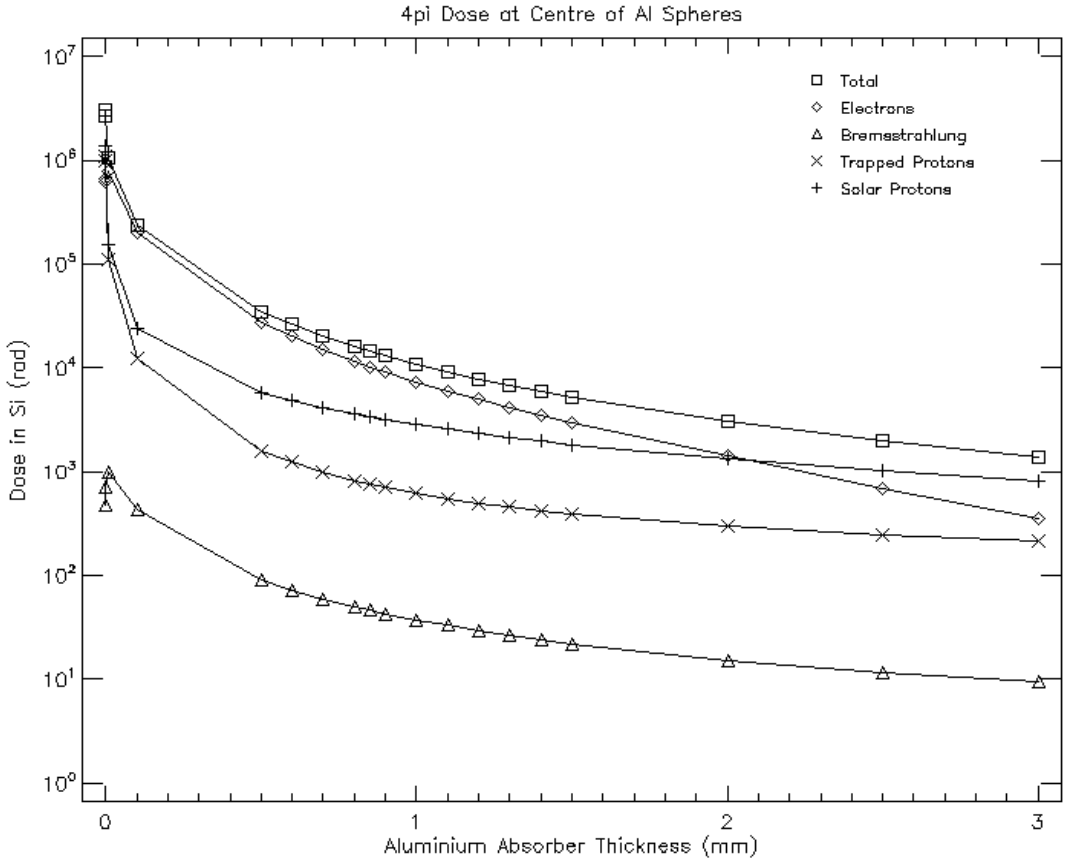

Figure 15: Dose of Si at the center of Al sphere for various thicknesses for a period of one year

3.5 Radiation variation

The magnitude of radiation varies depend on the altitude and inclination of orbit from the surface of the earth. The number of trapped particle and transient particle varies based on the altitude and inclination of the orbit. Since this mission operates in LEO orbit, the major ionizing dose is caused by trapped particles (proton and electron in Van Allen belt) and next the transient particle. To know difference in radiation level and particle fluence, the radiation model in spenvis is simulated at various orbital inclinations, for an altitude of apogee is 600 km and perigee is 400 km and with Al shielding of 2 mm thickness. The TID and particle fluence is estimated for different orbit inclinations, it is listed in the table: 11 &12 respectively.

Based on the results from simulation, TID absorbed by the silicon is higher in the poles and lower in the equator. As mentioned in theoretical section, the ionizing dose by electron is higher (3.75E+02 rad) near poles (60° to 89°) and lower in equator (1.46E+01 rad). The ionizing dose by trapped protons is higher in equator (2.58E-03 rad) and lower at poles (2.58E-03 rad). The ionizing doses by solar protons are zero in equator (0° to 30°) and higher in poles (1.32E+03). The values are listed in table: 11.

The numbers of electron is more at 60° (3.6×1013) and less in equator (3.89×10^{9}). The trapped protons are more than electrons in equator and lower in poles when compared to electron fluence. The solar proton (transient) fluence is null in equator and higher (3.15×10^{12}) in poles. GCR flux which is transient is higher in poles (6.78×10^{4}). The values are listed in table: 12. The main reason for higher ionizing dose at pole is due to more transient particles at poles. The transient particles are higher in poles due to lack of magnetic flux.

Table 12: TID variations for different orbit inclination at altitude of 600 to 400 km

Orbit inclination (°)	Al absorber thickness (mm)	Total Ionizing Dose (rad)	Bremsst -rahlung (rad)	Tapped protons (rad)	Trapped electrons (rad)	Solar Protons (rad)
0°	2	1.47E+01	1.18E-01	2.58E-03	1.46E+01	0.00E+00
28°	2	5.67E+02	2.13E+01	3.41E-01	5.45E+02	0.00E+00
60°	2	3.13E+03	2.42E+03	2.75E+01	3.75E+02	3.10E+02
89°	2	3.04E+03	1.40E+03	1.54E+01	3.03E+02	1.32E+03

Table 13: Particle fluence and GCR flux for different orbit inclination

Orbit inclination (°)	Al absorber thickness (mm)	Electron fluence (particles/cm^2)	Proton fluence (particles/cm^2)	Solar fluence (particles/cm^2)	GCR integral Flux (m^{-2} sr^{-1} s^{-1})
0°	2	3.89×10^{9}	2.89×10^{10}	0	4.79×10^{3}
28°	2	5.0×10^{11}	4.42×10^{11}	0	8.8×10^{3}
60°	2	3.6×10^{13}	7.66×10^{11}	7.39×10^{11}	4.6×10^{4}
89°	2	1.98×10^{13}	9.12×10^{11}	3.15×10^{12}	6.78×10^{4}

.

In this chapter the amount of dose would be exposed to the silicon in the orbit over a period of one year is estimated. The Total Ionizing Dose (TID) which should be irradiated to the device at radiation test facility is estimated, to ensure whether the component would survive in the orbit. In next chapter the process involved in radiation testing of the device and test plans are discussed.

4. Design of the radiation test setup

To measure and confirm the quality of COTS, irradiation testing is the only way. There are different source for irradiation. In this testing the Co_{60} gamma rays is used for the irradiation. The Co_{60} (gamma rays) radiative source are used for measuring the Total Ionizing Dose effects in the device. In analyzing most of the radiation test setup, generally the test setup is made in the research center or institutes which already has the radiation source and test facility for the testing the COTS components. One of the radiation facilities is available in ESTEC. The test facility available in the commercial market should be found. Once we found the test facility, according to that we could design the radiation test set up to perform radiation testing. The plan for the radiation testing is discussed in following.

4.1 Dose rate

The dose rate in space is not constant in the period of time. The mean dose rate in space is in the order of 0.0001 to 0.005 rad(Si)/s. During the time of solar flare the pulsed dose rate is in the order of 0.1 to 2 rad/s. But the mean dose rate very low to attain in the radiation test set up. It would take months to attain the TID if the mean dose rate is used for irradiation. The ESA/SCC 22900 has the standards for total dose steady-state irradiation test method. The dose rate classified into two levels;
Window 1 (Standard rate): 3.6 krad to 36 krad hr^{-1} (1 to 10 rad/s)
Window 2 (Low rate): 36 to 360 rad hr^{-1} (0.01 to 0.1 rad/s) [*ESASCC*] [*A. Barnard]* [*F. Sturesson*]

The standard rate is also known High dose rate; it is the most preferable one for COTS radiation test. High dose rate consumes less time and cost to attain the required TID. The cost for the production of Low dose rate is higher compared to the HDR and time taken for LDR to attain the TID is longer when compared to HDR. But the LDR almost creates the exact scenario in orbit and it's considered as the worst case scenario. In this radiation test the image sensor should able to operate without functional failure until the total dose of 5 Krad. [*Edmonds*]

The resistance of COTS components towards radiation differs highly with LDR and HDR. The components fail very earlier in Low dose rate when compared to High dose rate. Hence we prefer to perform both LDR and HDR test. But the first priority is LDR test. According to the ESA/SCC, the total exposure time should be less than 96 hrs. For the Low dose rate, the time constraint is considered. The CMOS components are preferred to do LDR test. There are two limiting factors in selecting the LDR. As the components should be reused after the irradiation, hence testing the component at 36 to 360 rad hr^{-1} has higher risk of destructing component at earlier stage of irradiation. Another factor is the time; based on convenience the test to be done in

a single day. Considering these two factors, intermediated dose rate 1 Krad/hr (0.27 rad/s) is decided. The dose rate of 1 Krad/hr will take 5 hr to reach total dose of 5 Krad.

4.2 Device under Test (DUT)

The testing can be done for a single component or in system level. Testing each component separately is reliable; it helps in finding the exact radiation effects in the component. In the initial phase each COTS component can be tested separately, in the latter phase radiation testing can be done in system level. To test a component, minimum of five random samples is needed. In which four samples are irradiated in testing and the fifth one is a reference sample, which is not irradiated but the functioning of the fifth sample is measured spontaneously. One of the four samples is in switch off state, to measure its radiation tolerance in switch off condition and remaining three is in on state.

The DUT is mounted on the test circuit board. The distance between DUT and the radiation source is determined by the dose rate and homogeneity of the desired radiation. The distance shall be three times the value of semi-diagonal of the test board or the illuminated beam should not exceed half cone angle of 18.4 deg. In the most of test setup the radiation source is fixed and test board is movable. The distance between the radiation source and test board is varied based on the required dose rate. The test board is placed closer to the radiation source if the required dose rate is higher and vice versa. The picture below shows the radiation source and test board setup. [*ESASCC*] [A. *Barnard*] [F. *Sturesson*]

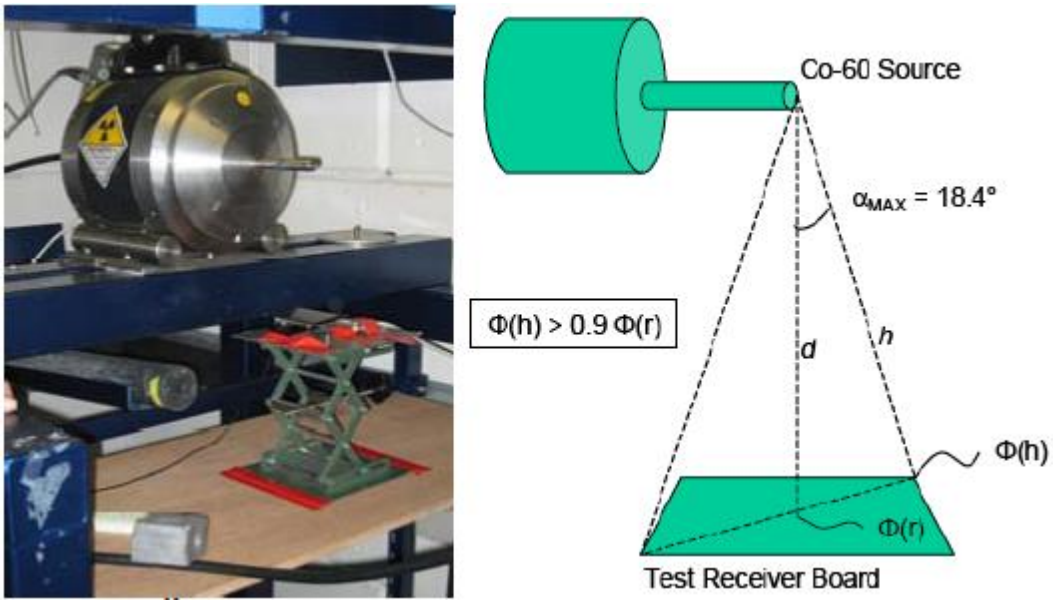

Figure 16: The Co60 radiation source [*Cecile*]

4.3 Radiation testing procedure

The radiation testing can be made in online or offline mode based on convenience. In online mode both irradiation of the device and the evaluation of the device are done in the same test setup and in offline mode irradiation and evaluation of the device are made in different places. In order to reduce the complexity of the shielding requirement of the measuring device both the parameters measurement and image quality assessment of the sensor are measured in offline mode the parameters are measured in a non radiative chamber at intermediate dose levels. The measurement is made at intermediate dose levels of 1, 2, 3, 4.5, 5 Krad. In the offline mode the measurement should be made within maximum of 1hr.

The radiation testing consists of three phase, (i) Pre-radiation testing, (ii) Radiation testing (iii) Post radiation testing (annealing). Throughout the test the components can be biased based on requirement, ESA/SCC specifies that biasing the components would create the worst case scenario. The biasing has different affect for different technologies of the component. Care full biasing should be made based on the technology. But the components tested under both biased and un-biased condition able to analyze the tolerance of the component in detail.

The electronic devices which monitor the DUT should be checked. The pre-radiation testing is the electrical measurement made before the irradiation. The parameters of the components are monitored, the monitored data is reported. The pre-radiation testing is done at room temperature. The second phase is the irradiation. The DUT is irradiated at the specified dose rate continuously until the component reach the specified dose of 5 Krad. The parameters of the components are monitored at intermediate dose level as explained before. The temperature during irradiation should be 20±10º C. The variation in temperature throughout the irradiation should not be more than 3º.

After the irradiation the third phase is the annealing. The annealing should begin within one hour of the completion of the irradiation. We recommend annealing of 168 hrs at 25º C. Annealing is the important process in radiation testing. After the required irradiation, the components are affected. The percentage of damage varies for different components. The components overcome the damage and come to stable condition during the annealing time. The components are evaluated during annealing, such that if the component would overcome the damage and regain its performance gradually. If the component fails during annealing then it's not validated. The whole radiation testing process is shown in the flow chart in fig:14. [*ESA/SCC*] [*Barnard*]

Test plan for approval of the components

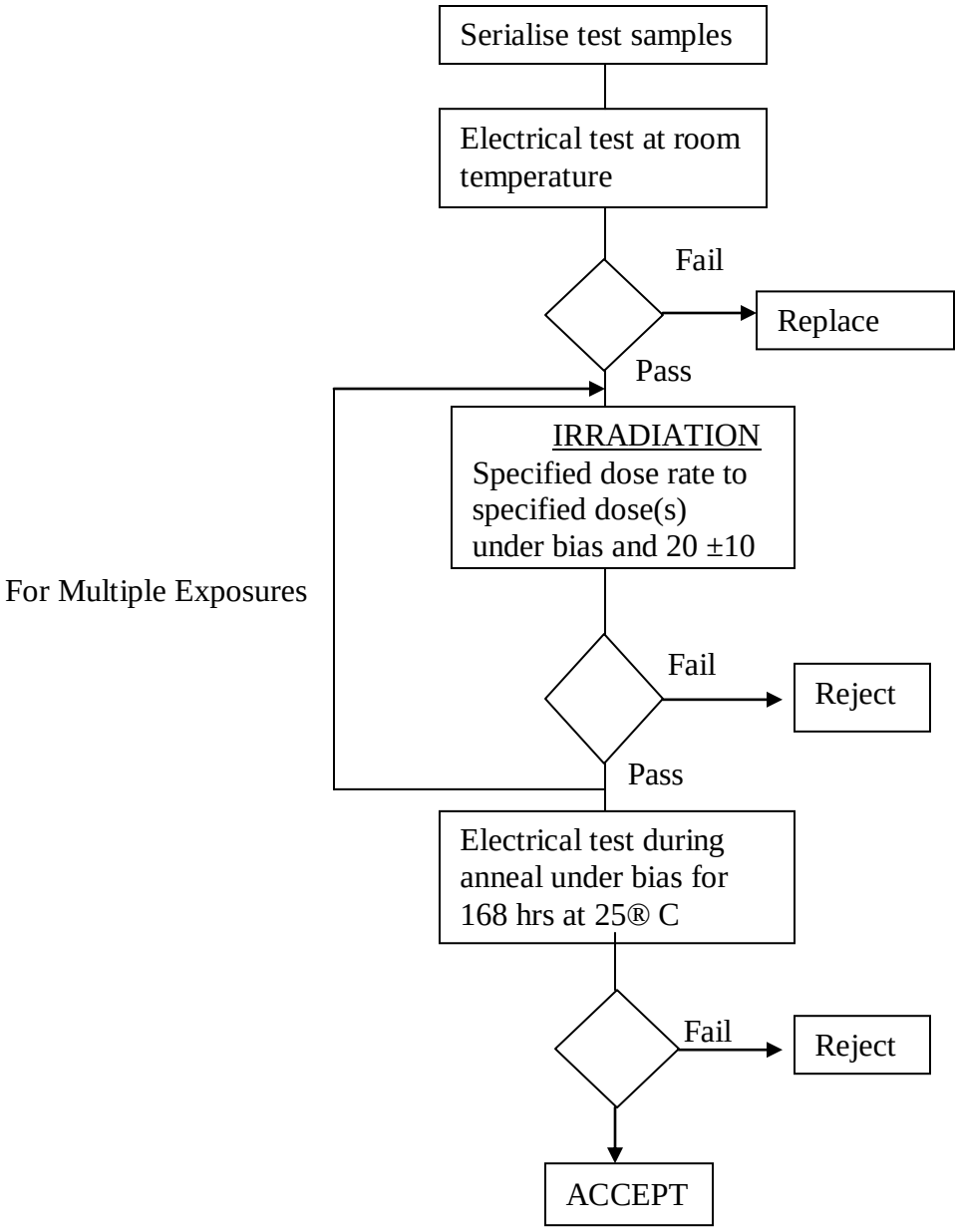

Figure 17: The test plan for testing TID of component

4.4 Test case

The main objective of the test is to measure the performance of the image sensor in radiation environment. The TID radiation test is planned to perform on PMD PhotonICs 19k-S3 image sensor (3D chip). The behavior of the sensor before irradiation, during irradiation, and after irradiation (annealing) will be measured. Two factors of sensor have to be observed during irradiation. First the parameters (ex: current consumption, power consumption, etc) of the sensor and second the pixel quality (ex: DSNU, PRNU and qualitative image assessment) of the sensor. These two factors have to be evaluated during and after irradiation to validate the image sensor. [*Chen*]

(i) Parameters measurement of the image sensor
(ii) Pixel quality assessment of the image sensor

(i) Parameters measurement of the sensor

The parameters of the sensor are measured during intermediate dose levels and after the irradiation (annealing). The parameters should not exceed its maximum values till the total dose of 5 Krad. If it exceeds then it's a functional failure, then the component is not approved to use in the orbit. The sensor parameters are specified in table: 13, these parameters show the performance of device. The pixel quality measurement is discussed in the next section. [*Torfs*] [*Johnston*] [*Bogaerts*]

Table 14: Senor Parameters

Parameters	Min.	Typ.	Max.
Current consumption		40 mA	50 mA
Power consumption		175 mW	225 mW
Supply voltage	4.9 V	5 V	5.1 V
Output current	-4mA		4 mA

(ii) Pixel quality assessment of the sensor

The characteristics of pixel is described in following;

- Dark current – When the image sensor is placed in a black box (not illuminated), there can be no current flow in an ideal sensor. But there is always leakage current produced by thermally generated charges in a real sensor, it is known as dark current. The dark current for a single pixel can be determined in a black box. The dark current per second is calculated, if the dark frames of the pixel are captured at several integration times.

- Quantum efficiency – Quantum efficiency is the sensor response to different wavelength of light. The number of photon incident on a pixel is compared to the number of electron produced.

QE (λ) = $N_{det}(\lambda) / N_{inc}(\lambda)$
N_{det} – detected signal charge per pixel at wavelength (λ)
N_{inc} – number of incident photons of wavelength (λ)

- Conversion gain - The sensor converts the photo-generated electron to micro voltage and the potential gain measured per electron is the conversion gain

- Dark Signal Non Uniformity (DSNU) and Photon Response Non-uniformity (PRNU) – These two properties describes the uniformity of each pixel in an array. The DSNU shows the distribution of dark current and leakage difference between the pixels. PRNU shows pixel responsiveness when illuminated and gain difference between the pixels.

The image sensor characterization is based on fill factor, quantum efficiency, conversion gain, full well capacity, dark current, noise parameters, integration/exposure time, and dynamic range. The dark current, quantum efficiency, and charge conversion gain are the main parameters, which are assessed from digital output data collected in dark and illuminated conditions. The function quantum efficiency and charge conversion gain is shown in the fig: 14. [*Wallis*] [*Goodbeer*]

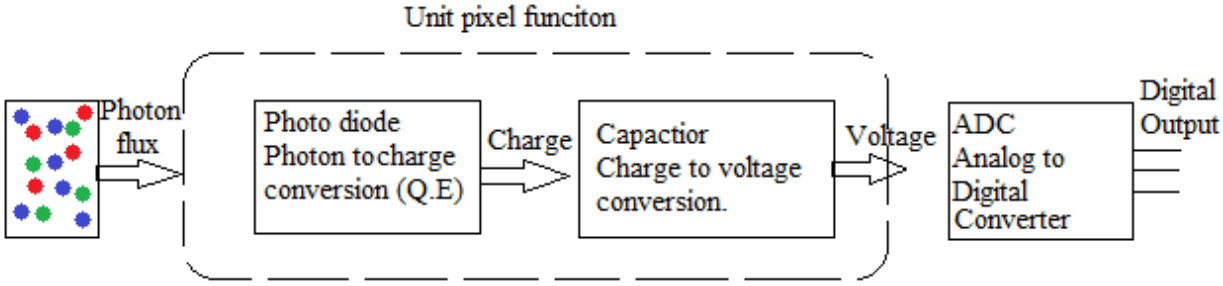

Figure 18: Image sensor function

Test methodologies:

The Radiation testing of PMD camera is made in system level. The test bench is designed to evaluate sensor parameters. The camera is placed inside a black box to collect the dark images. The equipments inside the black box are light source for flat field illumination and an object (ex: bar, cylinder, etc) for imaging. Thermocouples are placed inside a black box to measure the ambient temperature and sample temperature of the sensor. The data collection and sensor control are made using laptop interface.

The test can be performed by manual and auto settings in sensor. Most of the image sensors have on chip image correction features to provide to low noise performance. The function of auto correction features is to adjust the parameters of the sensor, it could mislead in measuring the

effects on parameters of the device during irradiation. For ex: the dark signal in pixel is increased with the TID, it could be changed by auto correction features. The main idea is to identify the basic degradation in the image senor without auto correction features (manual) and also to identify how the effects could be corrected using auto function enabled. The data from the images sensor can be collected in two ways, manual and auto. The manual data collection has fixed exposure time, fixed signal chain gains (analog to digital) and disabled on chip correction features. The auto method has data collection with sensor auto function enabled to know how the radiation effects are corrected internally by the sensor. [*Becker*] [*Thorbourn*]

The following data set are collected in pre and post radiation. Dark images collected at different integration time, it is used to for calculating dark signal rate, noise, dark signal non-uniformity (DSNU). Flat field images at different integration times to measure the photon transfer curve, noise, photo response non-uniformity (PRNU). Images of target object at best focus for different integration time, to measure the quality of the image, the distance between the sensor and the object. The auto data measure the same functions at one exposure time chosen by sensor with auto correction features. The fig.16 is an example for the test bench setup.

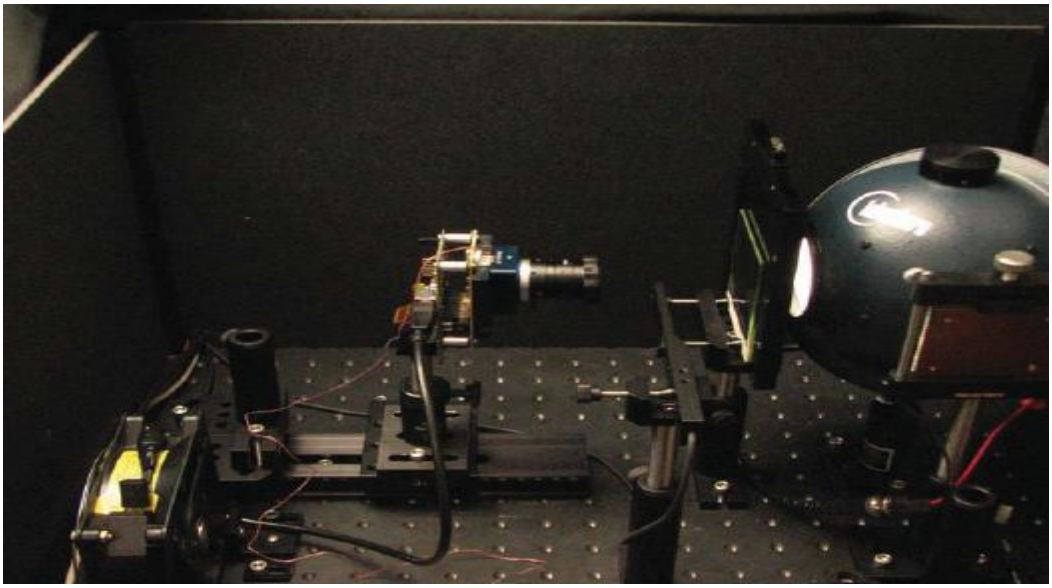

Figure 19: Commercial sensor survey test bench. [*Becker*]

i) Dark signal - The dark signal data (five set of frames) are collected under un-illuminated condition with same integration time from micro seconds to seconds. For the pre- irradiation, dark signal is captured relatively in longer integration time and high conversion gain. After the irradiation two sets of dark frames are collected, the one with same gain and integration time, another with less gain and less integration time. The average is calculated from the five set of frames on pixel basis. The mean dark rate is the difference of the average dark signal at two different integration times divided by the difference in time. To calculate dark signal rate

for entire array, the two post irradiation data sets has to be merged. The dark signal rate over entire image is calculated by averaging all the pixels.

ii) In another method the dark output voltage of the sensor is measured. The dark output voltage of each pixel is measured by placing the image sensor for certain integration time. The average value is calculated from relevant pixels in the array. Then average dark output voltage for various integration time is measured. The average dark output voltage Vs integration time is made. The slope of the straight line given dark signal (dark output voltage per unit time). The dark signal at various doses could be measured in this procedure. [*Eid*]

iii) DSNU: The dark signal non-uniformity is calculated for a pixel by dividing the array into 16×16 windows and rms dark rate value is calculated over each window.

iv) PRNU: Flat field images (illumination – LED light) is used to determine the photo response non-uniformity. The five set of frames are collected at same integration time and averaged. Photo response rate is calculated by the difference of the average for two integration times divided by difference in integration time.

v) Pixel Noise: The average rms pixel noise is calculated from the dark frame data.

vi) Target image (qualitative image assessment): The images are taken before and after irradiation for an exposure time of 200 ms. The auto correction feature should be enabled. The hot pixels in pictures will be recognized after the irradiation. The image quality is compared before and after irradiation.

vii) Gain: The data's are represented in digital number (Analog to Digital). The digital number is converted to electron by plotting the signal variance (DN^2) Vs average signal level under flat field illumination condition. The conversion gain is calculated for dark and illuminated data sets. [*Becker*] [*Vu*]

viii) Quantum efficiency: To measure the quantum efficiency, the (PRNU) method could be used with the light source of different wavelength (ex: LED) [*Gonthier*] [*Walkera*].

Table 15: Pixel Parameters

Parameters		Min.	Typ.	Max.
Quantum efficiency	10 MHz	40%	50%	
	20 MHz	30%	40%	
Dark current			150 fA	200 fA
Conversion gain		3.8µV/e	4.5 µV/e	

ix) Distance measurement: The above parameters measure the quality of the pixel under illuminated and dark condition; it's a grey scale value of the pixel. Another important property of the PMD image sensor is depth (distance measurement). The object of interest is placed in front of image sensor with a known distance. The distance can be varied from 0.1m to 7.5m (it's based on frequency modulation of sensor). Each pixel in the sensor measure the distance to the object. The measurements are made during irradiation or at each intermediated dose levels. By comparing the measured value of each pixel with the reference, the pixel performance in measuring distance will be evaluated.

5. Conclusion

In order to qualify the PMD image sensor for orbital operation, the following things have been done. First the theoretical study about radiation sources and effects. The trapped charged particles, solar events, Galactic cosmic rays are the major sources exposed to the target orbit. Their properties and their maximum exposure during the solar cycle are detailed. The radiation effects are classified into cumulative and Singe Event Effect. The Total Ionizing Dose and Displacement Damage come under cumulative effect. These two are major effects for image sensor. The Single Event Effect is classified into permanent effect and transient effects. Single Event Latchup effect occurs more in CMOS based devices. The information from the previous space mission implies that the total dose of 4Krad will be exposed on target orbit for duration of one year.

The SPENVIS software is used for radiation simulation. In the target orbit, the number of electrons is higher than the number or protons. The energy range of protons is higher than electron. The protons are mostly distributed over the south Atlantic region. The electrons are distributed mostly around the north and south poles. In comparing all the sources, GCR ions have the high energy. The simulation results show that the target material silicon (Si) shielded in Al sphere of thickness 2mm contains the following absorbed doses. The trapped electron is the main source of radiation, which produce dose of (1.40 Krad). The second main source is solar proton, it produce dose of (1.31Krad). The trapped proton has the dose of (3.03E+02 rad). The Bremsstrahlung produces the dose of (1.53E+01 rad). The Total Ionizing dose of the mission is (3.04E+03 rad).

The COTs component has a radiation tolerance of 1- 10 Krad and untested COTS component will survive up to 5Krad, this are initial assumptions. The value of 3.04 Krad is within the criteria of COTS dose limit. Hence the component without shielding should be irradiated in the radiation test facility up to the total dose of 5Krad. If the component would survive the irradiation without functional failure until 5Krad or at the least until 4.56 Krad (which is 1.5×3.04 Krad, it's based on RDM) then the component would probably survive in the orbit with shielding of 2mm for one year.

The intermediated dose rate 1 Krad/hr (0.27 rad/s) is decided. The dose rate of 1 Krad/hr will take 5 hr to reach total dose of 5 Krad. To test a component, minimum of five random samples is needed. In which four samples are irradiated in testing and the fifth one is a reference sample, which is not irradiated but the functioning of the fifth sample is measured spontaneously. One of the four samples is in switch off state, to measure its radiation tolerance in switch off condition. The remaining three samples are tested in on state, to know which two of the samples have similar results. The test plan for the approval of the component is discussed in detail. The testing can be made in a system level or in a component level, based on the convenience.

The next step is the test case, the ways to measure the performance of sensor during the testing is described. First factor, the parameters of the sensor is measured during intermediate dose levels and after the irradiation (annealing). The parameters should not exceed its maximum values till the total dose of 5 Krad. If it exceeds then it's a functional failure, then the component is not approved to use in the orbit. The second main factor is to measure the pixel quality of the senor. The dark signal, DSNU, PRNU, pixel noise, gain, quantum efficiency, qualitative image assessment and distance measurement are to be evaluated to measure the quality of sensor. The test methodologies to monitor these functions are described in detail. These two factors have to be evaluated during and after irradiation to validate the image sensor.

5.1 Future work

The main aim of the thesis was to implement the radiation testing but we could not acquire the required amount of samples for testing. According to the ESA specification for TID testing, 11 samples are required for testing. But a minimum of five samples is required to reach the desired radiation testing. In the worst case the test could be made in a system level with one sample but it cannot justify the testing. To know exact performance of the PMD image sensor 3D chip, the component level test should be made with minimum of five samples. In order to take next step towards testing, first we need minimum of five samples. Once the required samples are acquired then the PCB layout should be designed and manufactured. Then it should be programmed to control its function and to retrieve the data. The next step is to find the test facilities to perform the test. Then the required test setup to measure the parameters at test facility should be discussed in earlier to the test. Once these criteria are fulfilled the TID test will be achievable. Biasing the device and accelerated testing at high temperature can also be considered if it is needed. After the testing the results can be analyzed to estimate the radiation tolerance of the PMD image sensor.

The TID testing for image sensor is just a first level of radiation testing. The next important test for images sensor is Displacement Damage (non-ionizing test).The Displacement Damage can be simulated using SPENVIS. Once the TID, DD test are made the cumulative effects on sensor can be analyzed. After this SEE testing should be planned, the permanent and transient effect can be tested in particle accelerator. By these testing the radiation effects in the component can be known well.

Reference

1) European Cooperation for Space Standardization, Space Engineering- Methods for the calculation of radiation received and its effects and a policy for design margin, **ESA-ESTEC, May 2008.**

2) **ESA/SCC** basic specification No.22900. "Total Dose Steady-State Irradiation."

3) **A.Barnard**, and W.H. Steyn, Low cost TID testing of COTS components, IEEE, 2007.

4) **Becker N.Heidi, Dennis O. Thorbourn**. Commercial Sensor Survey . Pasadena: Jet Propulsion Laboratory, 2010.

5) **BeckerN. Heidi, Michael D. Dolphin**, Commercial Sensor Survey Radiation Testing Progress report, Pasadena: Jet Propulsion Laboratory, 2008.

6) **Bogaerts, J. B. Dierickx**, "Total Dose Effects on CMOS Active Pixel Sensors." Leuven, Belgium.

7) **Cecile Renaudie, Markus Markgraf**, Radiation Testing of commercial-off-the shelf GPS Technology for use on LEO satellites, IEEE, 2007.

8) **Chen Yuan, Steven M. Guertin**, A Chip and Pixel Qualification Methodology on Imaging Sensor, Pasadena: Jet Propulsion Laboratory.

9) **Eid El-Sayed, Richard H. Tsai**, Radiation-Induced Dark Signal in 0.5-Micron CMOS APS Image Sensors. Photonics for Space Environments VII, 2000.

10) European Cooperation for Space Standardization, Space Engineering- Calculation of radiation and its effects and margin policy handbook, **ESA-ESTEC, December 2010.**

11) **F.Sturesson**, Total Ionizing Dose Testing, EPFL space center, June 2009.

12) **F. Faccio** , COTS for the LHC radiation environment: the rules of the game. Geneva: CERN.

13) **Godbeer, Adam**, Investigation of 4T CMOS Image Sensor Design, University of Surrey, February 2010.

14) **Gonthier P.Martin, P.Magnan,** Overview of CMOS process and design options for image sensor dedicated to space application, Society of Photo-Optical Instrumentation Engineers, 2005.

15) **James R. Schwank,** Marty R. Shaneyfelt, Paul E. Dodd, Radiation hardness assurance testing of microelectronic devices and integrated circuit, New Mexico: Sandia national laboratories, 2008.

16) **Johnson Space Center (JSC)**, *S*pace radiation effects on electronic components in low-earth orbit. NASA- PRACTICE NO. PD-ED-1258, April 1996.

17) **Johnston Allan. H**, Steven M. Guertin, The effects of space radiation on linear integrated circuits, California: Jet Propulsion Laboratory.

18) Johnston Allan. H, **G M Swift**, Radiation Test Requirements for Ionization and Displacement Damage, JPL Documents D-18002, July, 1999.

19) **Kayali S. A**, A. H. Johnston. Reliability and radiation hardness of compound semiconductors. NASA, Jet propulsion laboratory.

20) **L.D. Edmonds**, C.E. Bames, L.Z. Scheick, An introduction to space radiation effects on microelectronics, Pasadena, California: Jet Propulsion Laboratory, May 2000.

21) **Lightsey E. Glenn**, Operation Considerations of Cubesats Beyond Low Earth Orbit. Massachusetts: icubesat workshop Cambridge, May, 2012.

22) **Lima Fernanda Gusmao de**. "Single Event Upset Mitigation techniques for programmable devices", Porto Alegre, December, 2000.

23) **R.Rerrario, R.Finotello**, "Stereo vision measurement system for low earth orbit applications." Italy, November, 2004.

24) **Richard H. Maurer**, Martin E. Fraeman, Mark N. Martin, David R. Roth. Harsh Environments: Space Radiation, Environment, Effects and Mitigation. Johns Hopkins APL Technical Digest, Volume 28, Number 1, 2008.

25) **Sakovsky Kiril**. Radiation Hardness Testing for space application electronic devices, PDI, 2012.

26) **Sanchez**, Karla Patricia Reyes, Radiation environment over the WFM detector in LOFT's ESA mission. Barcelona: Escola Tecnica superior d'engineyeria de telecomunicacio de Barcelona, May 2013.

27) **Space station program office (ISS)**. *Space station ionizing radiation design environment.* Houstan: Johnson Space Flight Center, June 1994.

28) SpenvisD . "http://www.spenvis.oma.be/help/background/shieldose/shieldose.html."

29) SpenvisD2 . "http://www.spenvis.oma.be/ecss/frame.php/e_st_10_12c/06_02_04."

30) SpenvisG. "https://www.spenvis.oma.be/help/background/gcr/gcr.html."

31) SpenvisS. " https://www.spenvis.oma.be/help/background/flare/flare.html."

32) SpenvisT. "www.spenvis.oma.be/help/background/traprad/traprad.html."

33) **Thorsten Ringbeck**, A 3D time of flight camera for object detection, BU systems, Germany , July 2007.

34) **Torfs Tom**, IRIS-3 Characterization Report, Part 2: Radiation Tests. ESA- ESTEC., October, 2003.

35) **Underwood Craig**, Experience of using COTS technology in space, UK: Surrey space center.

36) **Vu Paul, Boyd Fowler**, Design of Prototype Scientific CMOS Image Sensors, Milpitas: SPIE Astronomical Telescopes and Instrumentation, June 2008.

37) **Walkera Andrew,Tim Eatona**. The Gaia Challenge: Testing High Performance CCDs in large quantities. Photo-Optical Instrumentation Engineers, 2008.

38) **Wallis Thomas**, Testing and Characterisation of Image Sensors at RAL, University of Surrey, April 2008.

Acronyms

List of abbreviation used in the report

COTS	Commercial Off-The-Shelf
PMD	Photonic Mixer Device
TID	Total Ionizing Dose
GCR	Galactic Cosmic Ray
LEO	Low Earth Orbit
HEO	Highly Elliptical Orbit
GEO	Geostationary Earth Orbit
SEE	Single Event Effect
SEU	Single Event Upset
SEFI	Single Event Functional Interrupt
SEL	Single Event Latchup
SEB	Single Event Burnout
SEGR	Single Event Gate Rupture
SESB	Single Event Snap Back
SET	Single Event Transient
SED	Single Event Disturb
SEHE	Single Event Hard Error
MCU	Multiple Cell Upset
DD	Displacement Damage
NIEL	Non Ionizing Energy Loss
CCD	Charge-Coupled Device
CMOS	Complementary Metal Oxide Semiconductor
CTE	Charge Transfer Efficiency
LET	Linear Energy Transfer
MOSFET	Metal Oxide Semiconductor Field Effect Transistor
SRAM	Static Random Access Memory
DRAM	Dynamic Random Access Memory
RDM	Radiation Design Margin
LDR	Low Dose Rate
HDR	High Dose Rate

DUT	Device Under Test
DSNU	Dark Signal Non Uniformity
PRNU	Photo Response Non Uniformity
QE	Quantum efficiency
FWC	Full Well Capacity

Developments software and tools

(i) SPENVIS
(ii) MATLAB
(iii) MS Word

Spenvis Data

Table 16: AP 9 Integral proton spectra

Energy (MeV)	Total mission average flux (/cm2/s)	Total mission fluence (/cm2)
1.00E-01	6.33E+03	2.00E+11
1.50E-01	5.35E+03	1.69E+11
2.00E-01	4.53E+03	1.43E+11
3.00E-01	3.22E+03	1.02E+11
4.00E-01	2.33E+03	7.35E+10
5.00E-01	1.75E+03	5.51E+10
6.00E-01	1.37E+03	4.32E+10
7.00E-01	1.13E+03	3.57E+10
1.00E+00	8.04E+02	2.54E+10
1.50E+00	5.91E+02	1.86E+10
2.00E+00	4.59E+02	1.45E+10
3.00E+00	3.03E+02	9.54E+09
4.00E+00	2.05E+02	6.47E+09
5.00E+00	1.47E+02	4.64E+09
6.00E+00	1.10E+02	3.47E+09
7.00E+00	8.67E+01	2.74E+09
1.00E+01	5.43E+01	1.71E+09
1.50E+01	3.77E+01	1.19E+09
2.00E+01	3.02E+01	9.52E+08
3.00E+01	2.28E+01	7.20E+08
4.00E+01	1.84E+01	5.80E+08
5.00E+01	1.49E+01	4.70E+08
6.00E+01	1.24E+01	3.92E+08
7.00E+01	1.06E+01	3.35E+08
1.00E+02	6.77E+00	2.13E+08
1.50E+02	3.55E+00	1.12E+08
2.00E+02	1.96E+00	6.18E+07
3.00E+02	6.16E-01	1.94E+07
4.00E+02	0.00E+00	0.00E+00
5.00E+02	0.00E+00	0.00E+00

Table 17: AP 9 Differential proton spectra

Energy (MeV)	Total mission average flux (/cm2/MeV/s)	Total mission fluence (/cm2/MeV)
1.00E-01	2.09E+04	6.59E+11
1.50E-01	1.80E+04	5.68E+11
2.00E-01	1.54E+04	4.85E+11
3.00E-01	1.10E+04	3.46E+11
4.00E-01	7.37E+03	2.32E+11
5.00E-01	4.81E+03	1.52E+11
6.00E-01	3.08E+03	9.73E+10
7.00E-01	2.06E+03	6.48E+10
1.00E+00	8.43E+02	2.66E+10
1.50E+00	3.45E+02	1.09E+10
2.00E+00	2.29E+02	7.22E+09
3.00E+00	1.27E+02	4.00E+09
4.00E+00	7.76E+01	2.45E+09
5.00E+00	4.76E+01	1.50E+09
6.00E+00	3.03E+01	9.54E+08
7.00E+00	2.01E+01	6.35E+08
1.00E+01	8.00E+00	2.52E+08
1.50E+01	2.41E+00	7.61E+07
2.00E+01	1.25E+00	3.93E+07
3.00E+01	5.90E-01	1.86E+07
4.00E+01	3.96E-01	1.25E+07
5.00E+01	2.97E-01	9.37E+06
6.00E+01	2.15E-01	6.79E+06
7.00E+01	1.69E-01	5.34E+06
1.00E+02	1.04E-01	3.29E+06
1.50E+02	4.81E-02	1.52E+06
2.00E+02	2.57E-02	8.11E+05
3.00E+02	9.80E-03	3.09E+05
4.00E+02	3.08E-03	9.71E+04
5.00E+02	0.00E+00	0.00E+00

Table 18: AE 9 Integral electron spectra

Energy (MeV)	Total mission average flux (/cm2/s)	Total mission fluence (/cm2)
4.00E-02	2.93E+05	9.24E+12
1.00E-01	1.50E+05	4.74E+12
2.00E-01	7.43E+04	2.34E+12
3.00E-01	4.30E+04	1.36E+12
4.00E-01	2.51E+04	7.91E+11
5.00E-01	1.51E+04	4.77E+11
6.00E-01	1.00E+04	3.15E+11
7.00E-01	6.55E+03	2.07E+11
8.00E-01	4.63E+03	1.46E+11
1.00E+00	2.51E+03	7.91E+10
1.20E+00	1.31E+03	4.14E+10
1.50E+00	6.60E+02	2.08E+10
1.80E+00	3.49E+02	1.10E+10
2.00E+00	1.83E+02	5.77E+09
2.20E+00	1.07E+02	3.38E+09
2.50E+00	6.59E+01	2.08E+09
2.80E+00	4.54E+01	1.43E+09
3.00E+00	3.18E+01	1.00E+09
3.20E+00	2.28E+01	7.18E+08
3.50E+00	1.63E+01	5.15E+08
3.80E+00	1.18E+01	3.72E+08
4.00E+00	8.47E+00	2.67E+08
4.20E+00	6.06E+00	1.91E+08
4.50E+00	4.24E+00	1.34E+08
4.80E+00	2.92E+00	9.20E+07
5.00E+00	2.05E+00	6.46E+07
5.50E+00	1.15E+00	3.64E+07
6.00E+00	7.42E-01	2.34E+07
6.50E+00	4.28E-01	1.35E+07
7.00E+00	2.05E-01	6.47E+06

Table 19: AE 9 Differential Electron Spectra

Energy (MeV)	Total mission average flux (/cm2/MeV/s)	Total mission fluence (/cm2/MeV)
4.00E-02	2.99E+06	9.42E+13
1.00E-01	1.77E+06	5.59E+13
2.00E-01	5.35E+05	1.69E+13
3.00E-01	2.46E+05	7.75E+12
4.00E-01	1.40E+05	4.40E+12
5.00E-01	7.54E+04	2.38E+12
6.00E-01	4.28E+04	1.35E+12
7.00E-01	2.69E+04	8.47E+11
8.00E-01	1.64E+04	5.16E+11
1.00E+00	8.02E+03	2.53E+11
1.20E+00	3.69E+03	1.17E+11
1.50E+00	1.93E+03	6.09E+10
1.80E+00	9.54E+02	3.01E+10
2.00E+00	4.84E+02	1.53E+10
2.20E+00	2.34E+02	7.39E+09
2.50E+00	1.23E+02	3.89E+09
2.80E+00	6.83E+01	2.15E+09
3.00E+00	4.53E+01	1.43E+09
3.20E+00	3.08E+01	9.73E+08
3.50E+00	2.20E+01	6.93E+08
3.80E+00	1.57E+01	4.96E+08
4.00E+00	1.14E+01	3.61E+08
4.20E+00	8.47E+00	2.67E+08
4.50E+00	6.29E+00	1.98E+08
4.80E+00	4.37E+00	1.38E+08
5.00E+00	2.91E+00	9.19E+07
5.50E+00	1.31E+00	4.12E+07
6.00E+00	7.25E-01	2.29E+07
6.50E+00	5.37E-01	1.69E+07
7.00E+00	3.55E-01	1.12E+07

Table 20: ESP Psychic total fluence: solar protons

	Fluence at spacecraft		Model fluence at 1.0AU	
	Total mission fluence		Total prediction period	
Energy (MeV)	Integral (cm^{-2})	Differential (cm^{-2} MeV^{-1})	Integral (cm^{-2})	Differential (cm^{-2} MeV^{-1})
0.1	2.46E+11	1.64E+12	1.18E+12	7.98E+12
0.11	2.31E+11	1.42E+12	1.10E+12	6.92E+12
0.12	2.17E+11	1.23E+12	1.04E+12	5.99E+12
0.14	1.95E+11	9.56E+11	9.35E+11	4.65E+12
0.16	1.78E+11	7.61E+11	8.54E+11	3.70E+12
0.18	1.64E+11	6.22E+11	7.87E+11	3.03E+12
0.2	1.53E+11	5.20E+11	7.33E+11	2.53E+12
0.22	1.43E+11	4.44E+11	6.86E+11	2.16E+12
0.25	1.31E+11	3.58E+11	6.29E+11	1.74E+12
0.28	1.22E+11	2.96E+11	5.82E+11	1.44E+12
0.32	1.11E+11	2.36E+11	5.31E+11	1.15E+12
0.35	1.04E+11	2.03E+11	4.99E+11	9.86E+11
0.4	9.52E+10	1.62E+11	4.56E+11	7.90E+11
0.45	8.78E+10	1.33E+11	4.20E+11	6.46E+11
0.5	8.17E+10	1.11E+11	3.91E+11	5.40E+11
0.55	7.66E+10	9.47E+10	3.66E+11	4.61E+11
0.63	6.98E+10	7.56E+10	3.34E+11	3.67E+11
0.71	6.43E+10	6.17E+10	3.08E+11	3.00E+11
0.8	5.92E+10	5.04E+10	2.83E+11	2.45E+11
0.9	5.46E+10	4.13E+10	2.61E+11	2.01E+11
1	5.09E+10	3.45E+10	2.43E+11	1.68E+11
1.1	4.77E+10	2.94E+10	2.28E+11	1.43E+11
1.2	4.49E+10	2.55E+10	2.15E+11	1.24E+11
1.4	4.04E+10	1.97E+10	1.93E+11	9.60E+10
1.6	3.69E+10	1.57E+10	1.76E+11	7.64E+10
1.8	3.40E+10	1.28E+10	1.63E+11	6.25E+10
2	3.16E+10	1.07E+10	1.51E+11	5.22E+10
2.2	2.97E+10	9.16E+09	1.42E+11	4.45E+10
2.5	2.72E+10	7.40E+09	1.30E+11	3.60E+10
2.8	2.51E+10	6.41E+09	1.20E+11	3.12E+10
3.2	2.27E+10	5.82E+09	1.08E+11	2.83E+10
3.5	2.10E+10	5.22E+09	1.00E+11	2.54E+10
4	1.87E+10	4.07E+09	8.90E+10	1.98E+10
4.5	1.68E+10	3.26E+09	8.02E+10	1.58E+10
5	1.53E+10	2.83E+09	7.32E+10	1.38E+10
5.5	1.40E+10	2.53E+09	6.65E+10	1.23E+10
6.3	1.22E+10	1.94E+09	5.80E+10	9.44E+09

	Fluence at spacecraft		Model fluence at 1.0AU	
	Total mission fluence		Total prediction period	
Energy (MeV)	Integral (cm^{-2})	Differential (cm^{-2} MeV^{-1})	Integral (cm^{-2})	Differential (cm^{-2} MeV^{-1})
8	1.08E+10	1.59E+09	5.14E+10	7.73E+09
9	9.48E+09	1.31E+09	4.50E+10	6.36E+09
10	8.31E+09	1.02E+09	3.95E+10	4.95E+09
11	7.38E+09	8.54E+08	3.51E+10	4.15E+09
12	6.58E+09	7.36E+08	3.12E+10	3.58E+09
14	5.91E+09	6.08E+08	2.79E+10	2.96E+09
16	4.86E+09	4.43E+08	2.30E+10	2.15E+09
18	4.08E+09	3.41E+08	1.93E+10	1.66E+09
20	3.47E+09	2.65E+08	1.64E+10	1.29E+09
22	2.99E+09	2.12E+08	1.42E+10	1.03E+09
25	2.61E+09	1.75E+08	1.23E+10	8.50E+08
28	2.15E+09	1.31E+08	1.02E+10	6.36E+08
32	1.80E+09	1.02E+08	8.47E+09	4.98E+08
35	1.45E+09	7.39E+07	6.81E+09	3.59E+08
40	1.25E+09	5.95E+07	5.86E+09	2.89E+08
45	9.89E+08	4.35E+07	4.64E+09	2.11E+08
50	8.00E+08	3.22E+07	3.75E+09	1.57E+08
55	6.58E+08	2.45E+07	3.08E+09	1.19E+08
63	5.49E+08	1.92E+07	2.56E+09	9.32E+07
71	4.19E+08	1.33E+07	1.95E+09	6.49E+07
80	3.28E+08	9.50E+06	1.52E+09	4.62E+07
90	2.55E+08	6.78E+06	1.18E+09	3.30E+07
100	1.97E+08	4.79E+06	9.03E+08	2.33E+07
110	1.56E+08	3.42E+06	7.09E+08	1.66E+07
120	1.26E+08	2.47E+06	5.71E+08	1.20E+07
140	1.04E+08	1.89E+06	4.69E+08	9.20E+06
160	7.35E+07	1.20E+06	3.26E+08	5.82E+06
180	5.38E+07	7.72E+05	2.36E+08	3.74E+06
200	4.08E+07	5.28E+05	1.76E+08	2.51E+06
220	3.18E+07	3.77E+05	1.35E+08	1.76E+06
250	2.53E+07	2.78E+05	1.06E+08	1.29E+06
280	1.83E+07	1.85E+05	7.58E+07	8.40E+05
320	1.36E+07	1.27E+05	5.55E+07	5.71E+05
350	9.52E+06	7.82E+04	3.84E+07	3.44E+05
400	7.49E+06	5.67E+04	2.99E+07	2.45E+05
450	5.18E+06	3.58E+04	2.07E+07	1.50E+05
500	3.71E+06	2.33E+04	1.49E+07	9.53E+04
	2.78E+06	1.39E+04	1.12E+07	5.58E+04

Table 21: Ion spectrum (GCR)

Energy (MeV/n)	Integral flux (m2/ sr/ s/)	Differential flux (m-2 sr-1 s-1 (MeV/n)-1)
1.00E+00	1.05E+03	1.72E-04
1.10E+00	1.05E+03	2.08E-04
1.20E+00	1.05E+03	2.49E-04
1.40E+00	1.05E+03	3.40E-04
1.60E+00	1.05E+03	4.44E-04
1.80E+00	1.05E+03	5.61E-04
2.00E+00	1.05E+03	6.91E-04
2.20E+00	1.05E+03	8.32E-04
2.50E+00	1.05E+03	1.07E-03
2.80E+00	1.05E+03	1.33E-03
3.20E+00	1.05E+03	1.71E-03
3.50E+00	1.05E+03	2.02E-03
4.00E+00	1.05E+03	2.60E-03
4.50E+00	1.05E+03	3.22E-03
5.00E+00	1.05E+03	3.90E-03
5.50E+00	1.05E+03	5.93E-03
6.30E+00	1.05E+03	7.51E-03
7.10E+00	1.05E+03	9.23E-03
8.00E+00	1.05E+03	1.13E-02
9.00E+00	1.05E+03	1.38E-02
1.00E+01	1.05E+03	1.63E-02
1.10E+01	1.05E+03	1.91E-02
1.20E+01	1.05E+03	2.19E-02
1.40E+01	1.05E+03	2.78E-02
1.60E+01	1.05E+03	3.41E-02
1.80E+01	1.05E+03	4.06E-02
2.00E+01	1.05E+03	4.72E-02
2.20E+01	1.05E+03	5.41E-02
2.50E+01	1.05E+03	6.45E-02
2.80E+01	1.05E+03	7.50E-02
3.20E+01	1.05E+03	8.92E-02
3.50E+01	1.05E+03	9.98E-02
4.00E+01	1.05E+03	1.17E-01
4.50E+01	1.05E+03	1.34E-01
5.00E+01	1.05E+03	1.51E-01
5.50E+01	1.05E+03	1.67E-01
6.30E+01	1.05E+03	1.92E-01

Energy (MeV/n)	Integral flux (m2/ sr/ s/)	Differential flux (m-2 sr-1 s-1 (MeV/n)-1)
7.10E+01	1.05E+03	2.15E-01
8.00E+01	1.05E+03	2.39E-01
9.00E+01	1.04E+03	2.63E-01
1.00E+02	1.04E+03	2.85E-01
1.10E+02	1.04E+03	3.04E-01
1.20E+02	1.03E+03	3.22E-01
1.40E+02	1.03E+03	3.50E-01
1.60E+02	1.02E+03	3.74E-01
1.80E+02	1.01E+03	3.97E-01
2.00E+02	1.00E+03	4.17E-01
2.20E+02	9.96E+02	4.31E-01
2.50E+02	9.82E+02	4.45E-01
2.80E+02	9.69E+02	4.52E-01
3.20E+02	9.51E+02	4.58E-01
3.50E+02	9.37E+02	4.61E-01
4.00E+02	9.14E+02	4.60E-01
4.50E+02	8.91E+02	4.54E-01
5.00E+02	8.69E+02	4.43E-01
5.50E+02	8.47E+02	4.29E-01
6.30E+02	8.13E+02	4.07E-01
7.10E+02	7.82E+02	3.86E-01
8.00E+02	7.48E+02	3.64E-01
9.00E+02	7.13E+02	3.39E-01
1.00E+03	6.80E+02	3.25E-01
1.10E+03	6.48E+02	3.02E-01
1.20E+03	6.19E+02	2.81E-01
1.40E+03	5.67E+02	2.45E-01
1.60E+03	5.21E+02	2.14E-01
1.80E+03	4.80E+02	1.88E-01
2.00E+03	4.45E+02	1.67E-01
2.20E+03	4.13E+02	1.48E-01
2.50E+03	3.72E+02	1.26E-01
2.80E+03	3.37E+02	1.08E-01
3.20E+03	2.98E+02	8.86E-02
3.50E+03	2.73E+02	7.74E-02
4.00E+03	2.38E+02	6.28E-02
4.50E+03	2.10E+02	5.19E-02
5.00E+03	1.86E+02	4.35E-02
5.50E+03	1.66E+02	3.70E-02
6.30E+03	1.39E+02	2.93E-02

Energy (MeV/n)	Integral flux (m2/ sr/ s/)	Differential flux (m-2 sr-1 s-1 (MeV/n)-1)
7.10E+03	1.18E+02	2.39E-02
8.00E+03	9.83E+01	1.95E-02
9.00E+03	8.07E+01	1.57E-02
1.00E+04	6.64E+01	1.29E-02
1.10E+04	5.47E+01	1.06E-02
1.20E+04	4.50E+01	8.83E-03
1.40E+04	2.99E+01	6.29E-03
1.60E+04	1.90E+01	4.63E-03
1.80E+04	1.08E+01	3.50E-03
2.00E+04	4.63E+00	2.71E-03

Table 22: Technologies susceptible to TID effects

Technology category	**Sub categories**	**Effects**
MOS	NMOS PMOS CMOS CMOS/SOS/SOI	Threshold voltage shift, Decrease in drive current, Decrease in switching speed, Increased leakage current.
BJT		hFE degradation, particularly for low-current conditions
JFET		Enhanced source-drain, leakage currents.
Analogue microelectronics (general)		Changes in offset voltage and offset current, Change in bias current, Gain degradation.
Digital microelectronics (general)		Enhanced transistor leakage, Logic failure from (1) reduced gain (BJT), or (2) threshold voltage shift and reduced switching speeds (CMOS)
CCDs		Increased dark currents, effects on MOS transistor elements (described above), some effects on CTE.
APS (CMOS)		Changes to MOS-based circuitry imager (as described above) – including changes in pixel amplifier gain**.**
MEMS		Shift in response due to charge build-up in dielectric layer near to moving parts.
Quartz resonant crystals		Frequency shifts
Optical materials	Cover glasses, Fiber optics, Optical components, coatings, instruments and scintillators.	Increased absorption, Variation in absorption spectrum (coloration).
Polymeric surfaces (generally only important for materials exterior to spacecraft)		Mechanical degradation, Changes to dielectric properties.

[*ESA2008*]

Table 23: Technology susceptible to DD effects.

Technology category	**Sub-category**	**Effects**
General bipolar	BJT Integrated circuits	hFE degradation in BJTs, particularly for low-current conditions (PNP devices more sensitive to DD than NPN)
	diodes	Increased leakage current and increased forward voltage drop
Electro-optic sensor	CCDs	CTE degradation, Increased dark current, Increased hot spots, Increased bright columns, Random telegraph signals.
	APS	Increased dark current, Increased hot spots, Random telegraph signals, Reduced responsivity.
	Photo diodes	Reduced photocurrents, Increased dark currents.
	Photo transistors	hFE degradation, Reduced responsivity, Increased dark current.
Light- emitting diodes	LEDs (general)	Reduced light power output
	Laser diodes	Reduced light power output, Increased threshold current.
Opto-couplers		Reduced current transfer ratio
Solar cells	Silicon, GaAs, InP, etc.	Reduced current short-circuit current, Reduced open-circuit voltage, Reduced maximum power.
Optical materials	Alkali halides, Silica.	Reduced transmission
Radiation detectors	Semiconductor gamma ray and X-ray detectors: Si, HPGe, CdTe, CZT.	Reduced charge collection efficiency (calibration shifts, reduced resolution), Poorer timing characteristics, HPGe show complex variation with temperature.
	Semiconductor charged-particle detectors.	Reduced charge collection efficiency (calibration shifts, reduced resolution)

[*ESA2008*]

Table 24: Definition of DD effects.

Parameter	Phenomenology and observation	Technologies affected
Charge-transfer efficiency (CTE)	Creation of traps in active volume of CCD – reduced charge collection form each pixel, also streaking observed due to the delayed release of trapped charge.	CCD
Dark current	Excess charge from electro-optic sensor due to charge collection from radiation-induced defects.	CCD, APS, photo-diodes, photo-transistors.
Hot spots	Defect-induced charge generation in specific pixels which become brighter than the average dark current. These are usually defined in the context of the application and identified by the image processing software as "bad pixels". Very bright spots can result from field- enhanced emission mechanisms.	CCD, APS.
Random telegraph signals (RTS)	Two or more multi-level dark –current states with random switching between the dark current states from seconds (for imager at room temperature) to hours (if operated at reduced temperature)	CCD, APS.
Bright columns	Defect-induced dark current can saturate a pixel with a time-constant comparable to or longer than device read out times. Information from one or more pixels after the damage pixel are this rendered unreadable**.**	CCD
Reduced photo-current, Pixel responsivity	Reduced charge collection as a result of decreased minority carrier life-times**.**	APS, photo-diodes, photo-transistors
Light output	Reduced radiation power efficiency.	LED, laser diodes.

[*ESA2008***]**

Table 25: Possible single event effect as a function of component technology and family

Component type	Technology	Family	Function	SEL	SESB	SEGR	SEB	SEU	MCU/SMU	SEDR	SEHE	SEFI	SET	SED
Transistor	Power MOS					X	X							
ICs	CMOS or BiCMOS or SOI	Digital	SRAM	X *				X	X		X			
			DRAM/SDRAM	X *	X			X	X		X	X		
			FPGA	X *				X		X		X		X
			EEPROM/ Flash EEPROM	X *						X		X		X
			µP/ µcontroller	X				X			X	X		X
		Mixed Signal	ADC	X *				X				X	X	X
			DAC	X *				X				X	X	X
		Linear		X *						X			X	
	Bipolar	Digital						X					X	
		Linear						X					X	
Opto-electronics			Opto-couplers										X	
			CCD										X	
			APS (CMOS)	X									X	
*except SOI														

[*ESA2008*]